NASA TT F-12,328

INVESTIGATION OF THE EFFECT ON PLASMA STRUCTURE IN CASE OF IMPACT OF AN ENERGY ENRICHED MICROPARTICLE

Hagen Dietzel

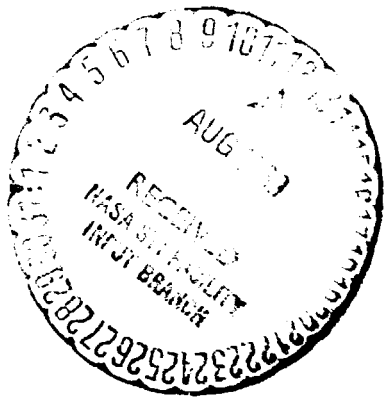

Translation of "Untersuchungen des Effektes der Plasmabildung beim Aufschlag energiereicher Mikropartikel"
Max Planck Institut für Kernphysik, Heidelberg, 1969, 41 pages

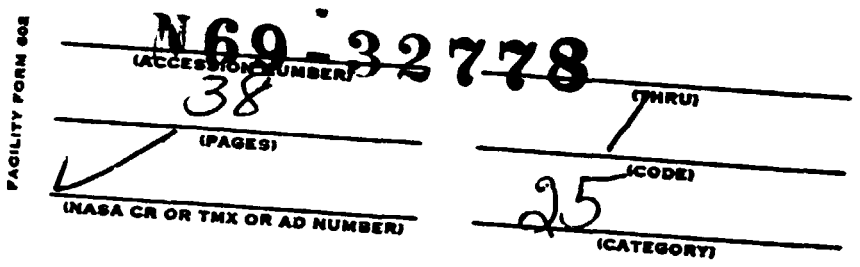

NATIONAL AERONAUTICS AND SPACE ADMINISTRATION
WASHINGTON, D. C. 20546 AUGUST 1969

Contents

NASA TT-F-12,328

INVESTIGATION OF THE EFFECT ON PLASMA STRUCTURE IN CASE OF IMPACT OF AN ENERGY ENRICHED MICROPARTICLE

Hagen Dietzel
Max-Plank Institute for Nuclear Physics, Heidelberg, Germany

ABSTRACT. Certain aspects of plasma formation by impact of high-energy cosmic particles on metal surfaces are investigated as a guide to future flight experimentation, including a a charge liberated as a function of particle charge, surface conditions, charge-separating field and angle of incidence. A Van de Graaf generator was used.

I. Introduction

Research on cosmic dust is important for several reasons. Someday we /1* shall have to organize the origin (that is the productive processes) and the history of solar system material into as comprehensive a theoretical picture of the solar system as possible. In addition a knowledge of space distribution and of the mechanical parameters of mass and velocity of these particles can also be of significance for the technical execution of space flight within the planetary system.

In order to approach clarification of the question of the origin and history of cosmic particles, knowledge of certain conditions are necessary. These include:

a) Particle occurrence;
b) Distribution of magnitudes of interplanetary particles;
c) Distribution of velocity of the particles in respect to direction and and amount;
d) Chemical composition of the particles.

The dependence of some of these magnitudes on distance from the sun and distance to the ecliptic is of great interest for the theoretical picture of the solar system in question. However, because of extreme expense, experimental research must often be limited to the neighborhood of the earth. Then the determination of the particle flow to the earth provides data about the occurrence and properties of cosmic particles in the neighborhood of the earths orbit. In order to get experimental data providing inferences about some of the above mentioned magnitudes, several paths may be followed: measurements of zodiacal light [1]; searches for micrometeorites in polar ice or in deep sea sedimentation and investigation of their chemical composition [2]; radar measurements [3], which are limited to particles with diameters $D \geqslant 1mm$ as their objects; finally experiments in collecting and recording [4].

Collecting experiments on rockets or satelites have the disadvantage that additional salvage of the collecting surfaces is necessary. Consequently this

*Numbers in the margin indicate pagination in the foreign text.

method is practically found only in the vicinity of the earth, and here chiefly in rocket flight. It has the advantage that once the particle is recognized as cosmic, it can be subjected to chemical analysis in the laboratory. In addition, investigations about the microcraters, possibly produced by impact, can be undertaken and compared with results of simulation tests [5]. However, [6] will indicate the difficulties in recognizing the cosmic origin of particles. /2

The principle of the method of registration consists of the direct use of the reciprocal action of the particle with a suitable sensor (measuring transformer). It transforms characteristic magnitudes of this reciprocal action, which depends on the particle parameters, into electrical signals which can be transmitted to the receiving station on earth by telemetry. Possible sensors of this type are: reflecting plates which are sensitive because of mechanical contact with a piezoelectric crystal element (microphones); thin plastic foils, metallized on both sides and provided with electrical potential; photomultipliers and combinations of them. Measuring results from flight experiments with some of these sensors are given in [4].

A further possibility for recording cosmic dust is given by an effect which is investigated in the laboratory [7] and [8] and used in a flight experiment in [9]: the formation of free charge carriers on the impact of energy enriched microparticles upon metal sufaces. Here charges of both polarities are liberated and form a plasma for periods of about 10^{-6} seconds in front of the place of impact. The charges in this plasma cloud originating in impact can be divided with the help of an electrical field, because the number of charge carriers is rapidly diminished by diffusion. The amount of charge is then measurable by a charge sensitive preamplifier. It is shown that the number of liberated charge characters depends on the mass and velocity of the projectile.

In the present work certain aspects of this plasma formation were investigated more exhaustively with reference to further application of the effect in flight experiments. It was to be determined whether, in addition to the mechanical projectile properties m and v, there are other parameters which influence the amount of liberated charge. Thus it was expedient to make a quantitative investigation of the following conditions in addition to the (m, v) dependency: /3

1. Dependence of the amount of charge liberated upon particle impact on the charged state of the projectile;
2. Dependence on the condition of the surface of the target (pretreatment, purity);
3. Dependence on the condition of the charge-separating field;
4. Dependence on the angle of incidence of the particle.

Since in many flight experiments screening from an exterior plasma is necessary, it also appeared in order to determine

5. The influence of special foils potentialized in front of the detector on the mechanical parameters m and v of the particle, and thus on the charge emmission upon impact.

The experiments of this work were carried out on a 2MV Van de Graaf particle accelerator. As projectiles which were supposed to stimulate cosmic dust, use was made of Fe particles of which the mass and velocities were included with the following limits.

$$10^{-15}\ g < m < 5 \times 10^{-10}\ g$$
$$0{,}8\ km/sec < v < 40\ km/sec$$

In almost all of the experiments the initial material used was tungsten, which according to [8] is also suitable for use in a flight experiment.

2. Experimental Procedures

/4

2.1. Acceleration of Microparticles

For the production of microparticles of high velocity we used a 2MV Van de Graaff particle accelerator which is provided with a special particle source [10, 11]. Fe particles with diameters of about 0.05 to 5 μ were used as particle material. These particles were provided constantly by a reservoir, charged positively[1] at a thin metal point and focused into the acceleration tube where they passed through the electrostatic potential produced by a band generator. In this way we obtain a particle beam of which the mass and velocity distributions depend upon the acceleration voltage, the mass distribution of the available particles and their charge. After the acceleration process the particles fly through two cylinder condensers. These measure the charge of the individual particles and their course between two fixed locations (the entry plane of the condensers). Before the opening of the cylinder condensers grids are set up and guard against influence from charges outside of the interior of the cylinder. In this way the entry and exit points of time of the particles, and thus a velocity measurement, is exactly defined. In accord with the equations

$$q\ U_B = (1/2)\ m\ v^2 \quad \text{and} \quad v = L/t_L$$

q = Particle Charge
U_B = Acceleration Voltage
t_L = Time Interval for Distance L

the mass m and the velocity v of a single particle are determined. The detection limit for q under normal operating conditions of the cylinder detectors lay at 5×10^{-15} Coulombs. In experiments with particles with a velocity exceeding 10 km/sec a greater charge sensitivity was necessary.

It was reached in the initial stage of the charge-sensitive preamplifier by decreasing static through transistor cooling. The smallest demonstrated /5

[1]The positive charge proves to be advantageous, because with a negative charge electrons are emitted as a result of the field admission, even with rather low surface field strengths (i.e. surface charge) of the iron particles.

charge lay between 4×10^{-16} Coulombs.

In many experiments the requirement was often present to permit only definite projectile parameters. Thus, the approximate conditions

$$q_0 < q < q_0 + \Delta q \quad ; \quad v_0 < v < v_0 + \Delta v$$

had to be fulfilled. Then the desired particles had to be separated from the still non-uniform particles provided by the accelerator. This is done by an electronic treatment of the detector signals. Particles of which the parameters do not fall within a two dimensional (q, v) interval selected by the experimenter can be guided out of the experimental beam by using this so-called dust filter after passing the analyzing detectors through a short sweep voltage which can be switched on [12]. A supplementary measurement of the charge and a further flight time control, however, are still required. In the first place the (q, v) interval cannot be made arbitrarily narrow for statistical reasons, because the waiting time for a suitable particle increases with an increase in the abruptness of the interval. In the second place the particle filter is overcharged under certain situations: thus, e.g. particles which follow each other within a time period $t < t_0$, cannot be separated. Here t_0 is the length of the high voltage pulse on the plates of the electrostatic sweep system.

Figure 1a gives a survey of the connection between the mass of a particle and the velocity which this particle reaches after passing through a prescribed acceleration voltage. From the relationships

$$q\ U_B = (1/2)\ m\ v^2$$

$$q = 4\pi r^2 \varepsilon_0 E$$

$$m = (4\pi/3)\ r^3 \rho$$

U_B = Acceleration Voltage
q = Particle Charged
m = Particle Mass
v = Particle Velocity
r = Particle Radius
E = Surface Field Strength on the Particle
ρ = Density of the Projectile Material

it follows that:

$$v = C\ m^{-1/6} \qquad \text{(Eq. 1)}$$

$$C = \sqrt{\left\{\frac{4}{3}\ \frac{\pi}{\rho^2}\right\}^{1/3} 6 \varepsilon_0 E\ U_B}$$

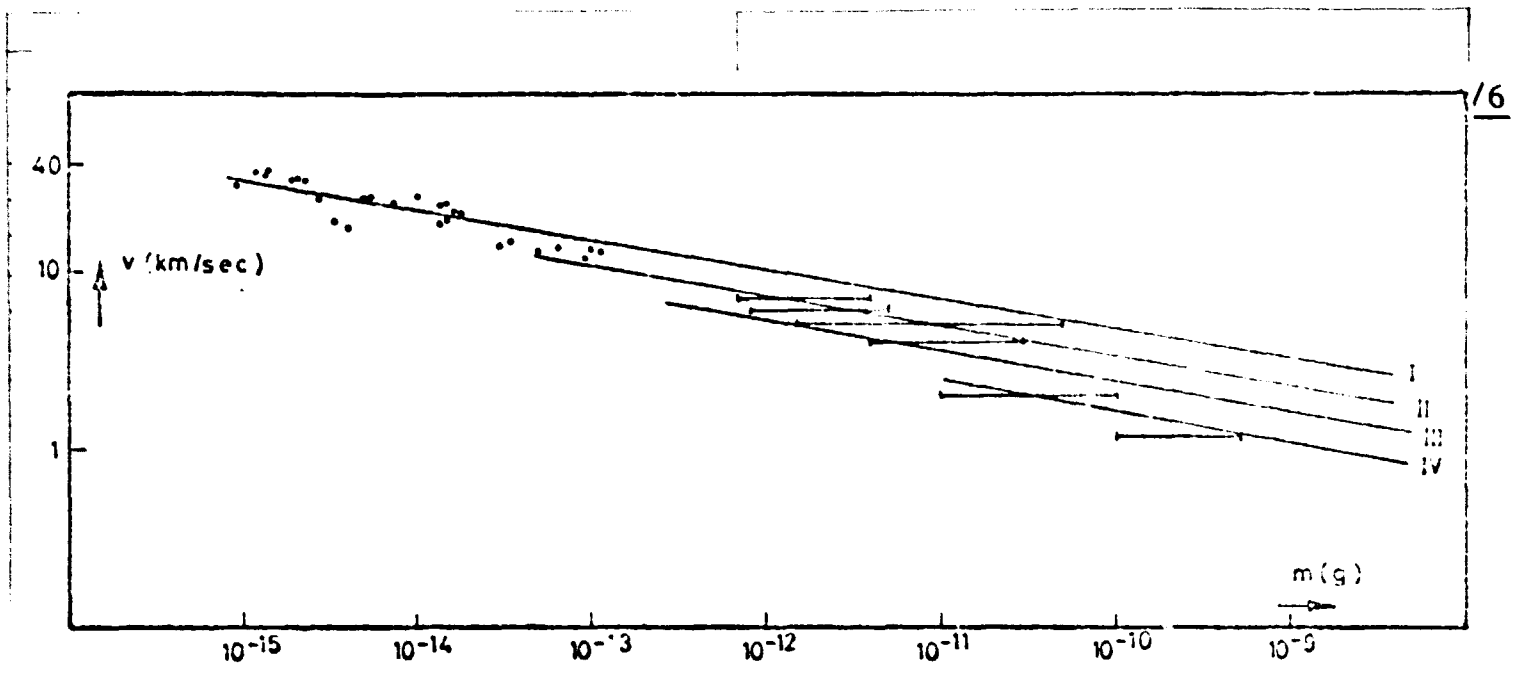

I: U_B=2MV II: U_B=1MV III: U_B=0.5MV IV: U_B=0.25MV

Figure 1a. The Mass Velocity Diagram of the Electrostatically Accelerated Fe Particles.

Curves I, II, III, and IV are computed according to Equation 1 and agree with the empirical data of the particle accelerator. In computing the curves for the surface field strength E, the value 2.5×10^7 V/m was introduced as a statistical mean value, which is reasonable according to [10]. E is subjected to a certain random variation. This results in the fact that an available particle with a mass distribution of finite width occurs, even when U_B is constant with a firmly chosen velocity. Such distributions are represented in Figure 1b.

2.2. Methods of Measurement /7

In this work each individual measurement is characterized by a triple value (m, v, Q). The determination of the mass and of the velocity v took place, as mentioned above, from the measurement of the charge and travel time of the particle. The charge Q liberated by the impact was identified at an electrically prestressed collecting electrode (usually a plane grid in front of the target surface) with the help of a charge-sensitive preamplifier and determined quantitatively. In order to obtain reasonable triple values, it came down to the point of storing information obtained before impact about the pair of parameters (m, v) until the measurement of the pertinent Q value had been made. This was essentially achieved through two different methods.

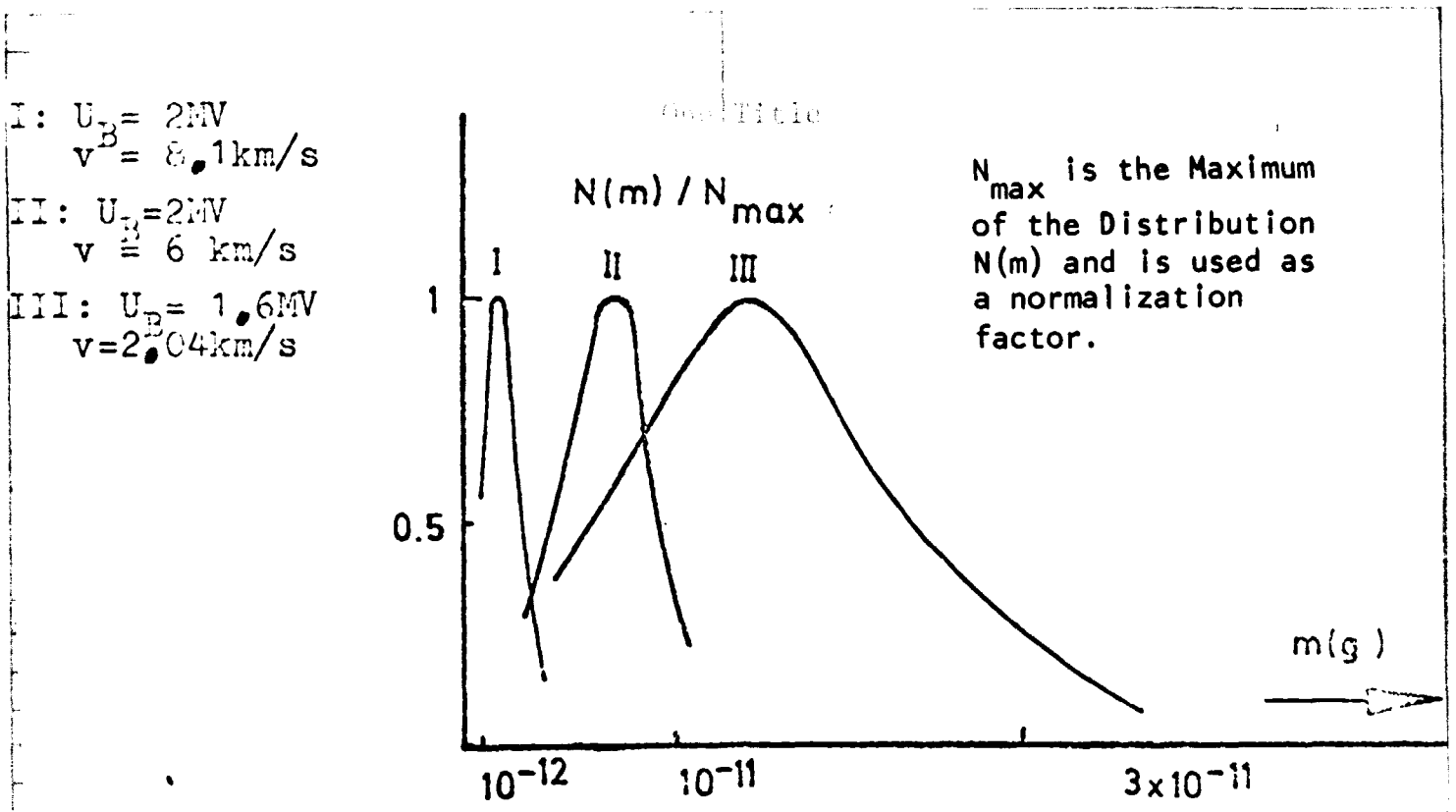

Figure 1b. Mass Distributions.

The first consisted of observing the signals for particle charging, liberated charge and travel time of the particle to a multi-beam oscillograph, where the various beams started out at the same time as entry into the control detector. These observations were obtained by photograph. The principle of this procedure is represented in Figure 2 (page 7).

In the second method a two dimensional, multi-channel analyzer was used (see block diagram in Figure 3, page 8). By choosing a constant velocity interval as narrow as possible, a two dimensional spectrum could be produced with the help of the particle filter. In this spectrum the charge of the particle (which is proportional to the mass of the particle for U_B and V = = const.) and the charge produced by the impact are stored up. The supplementary coincidences and flight time controls visible on the block diagram were necessary to eliminate errors in the spectrum. Such errors would be possible by altering the velocity of the particle between separation and impact through bands to the grid wires or through the fact that the particle filter does not separate particles following each other rapidly (see 2.1.). It is visible from the block diagram that cases with such erroneous velocity information are not considered in the spectrum. It should still be mentioned that when a multi-channel analyzer is used, the information on the shape of the pulse, i.e. the temporal process of charge production and subsequent diffusion and charge separation by means of the electrical field applied from outside vanishes.

a) Test Arrangement

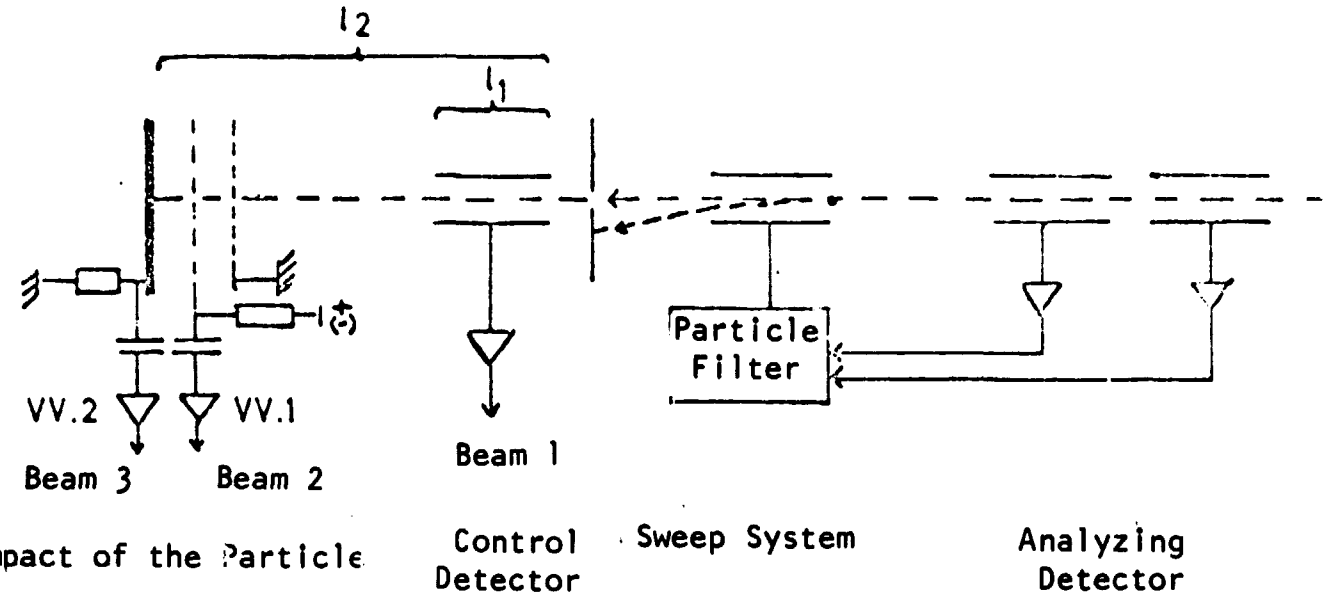

b) Temporal Process of Signals 1, 2 and 3

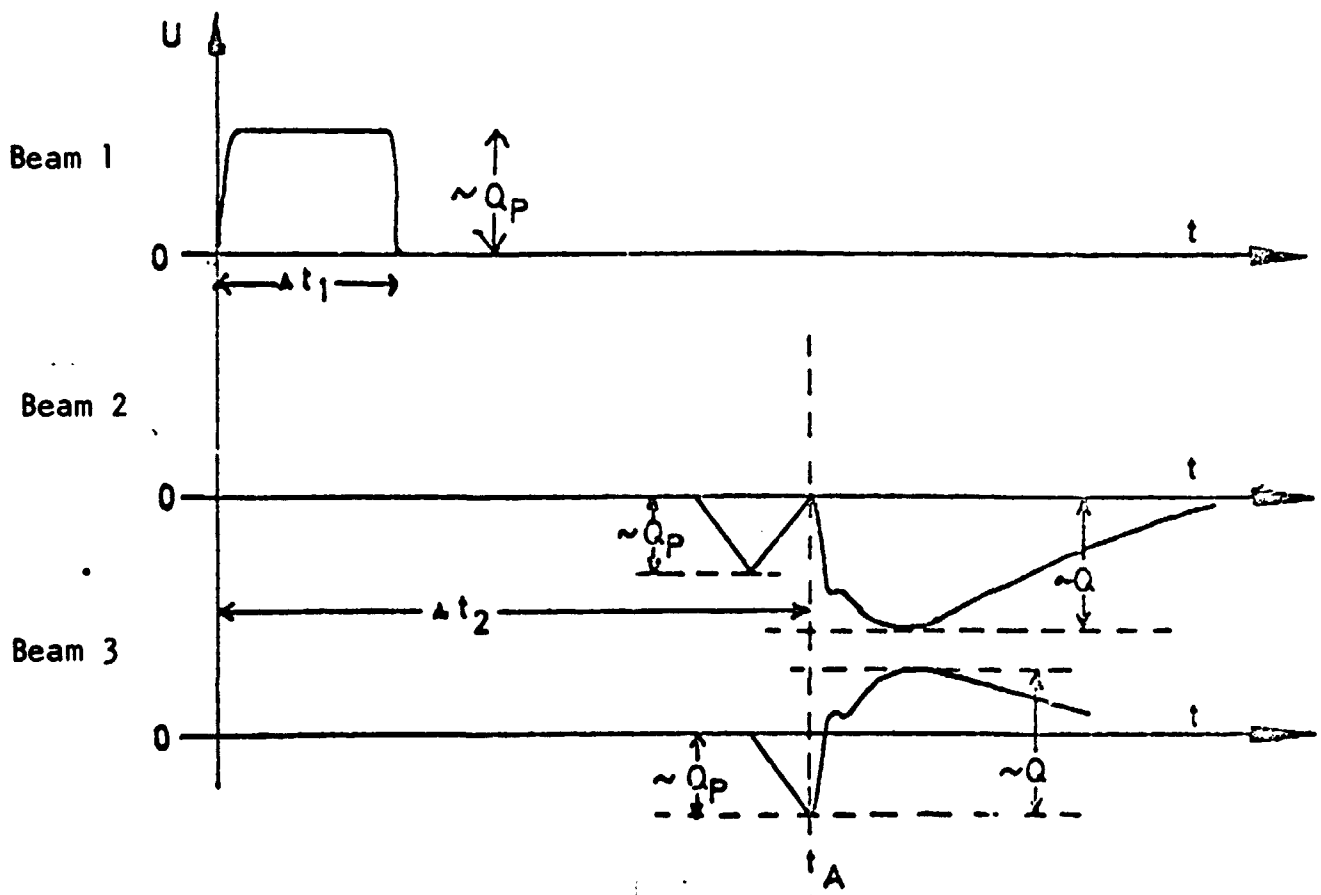

Figure 2.

Q_p Particle Charge

$\sim Q$ Charge Liberated Upon Impact

t_A Time Point of Impact

t_1 Flight Time for Distance l_1

t_2 Flight Time for Distance l_2

BLOCK DIAGRAM

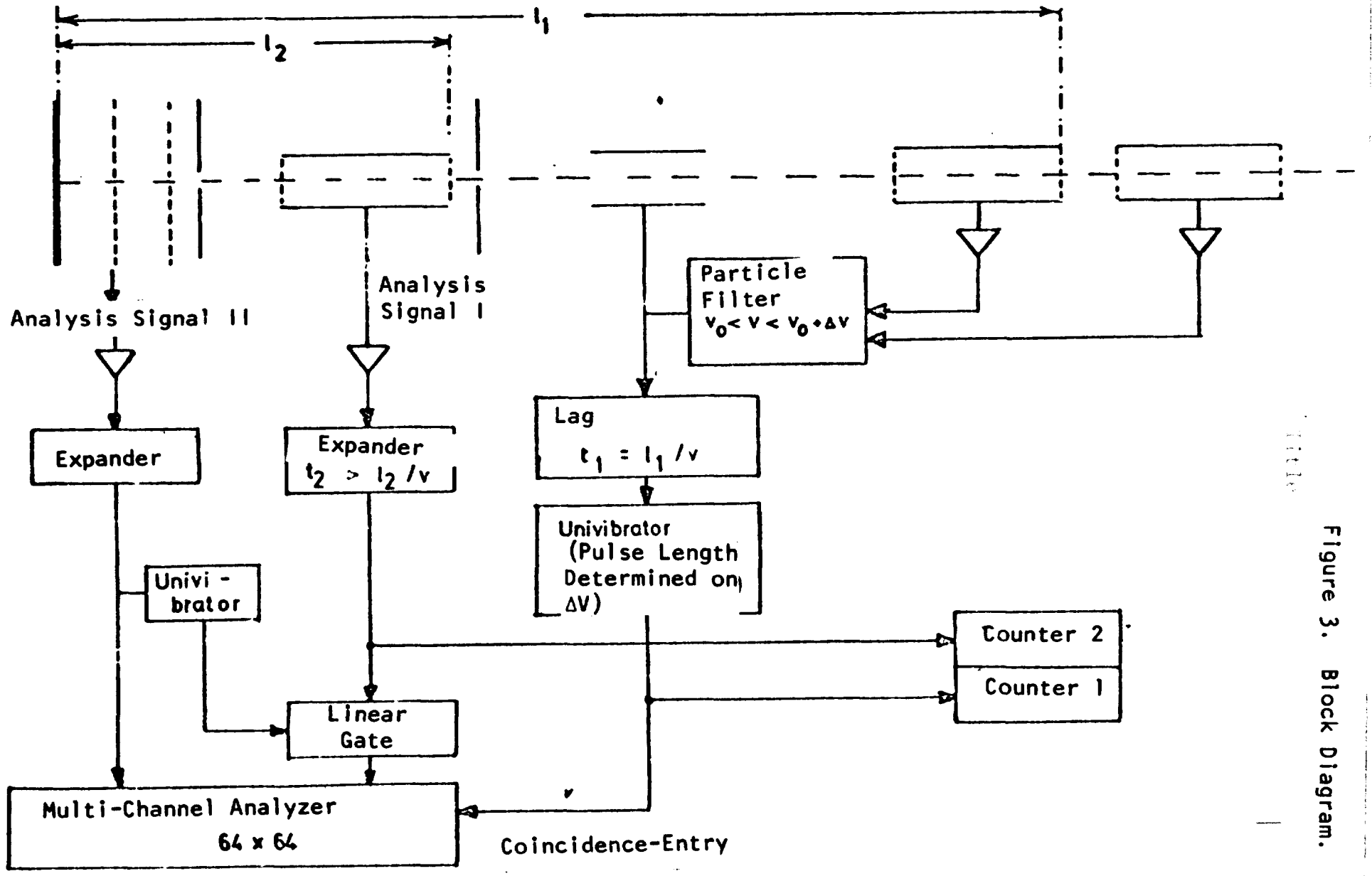

Figure 3. Block Diagram.

/7b

3. Measurements and Results

3.1. Preliminary Investigation: Influence of Particle Charge on Amount of Charge Freed by Impact /8

As already mentioned, the Fe projectiles carry a positve charge. To be sure in the manner described above this was used to accelerate and record the particle but in the present experiment it is no longer desirable for the particle to impact against the target. This is because we wish to express the effect of plasma formation in flight experiments in a statement about mass and velocity independent of whether the particle is charged or not. This is possible in a simple way if the amount of charge liberated proves to be independent of the charge conditions of the particle. This condition was tested in various experiments where the independence of the particle emission from the projectile particle was confirmed within the limits of error.

Figure 4a shows the results of an experiment in which the mass dependence of the charge emission was compared at constant velocity for different acceleration voltages. Particles which corresponded in mechanical parameters then carried different charges.

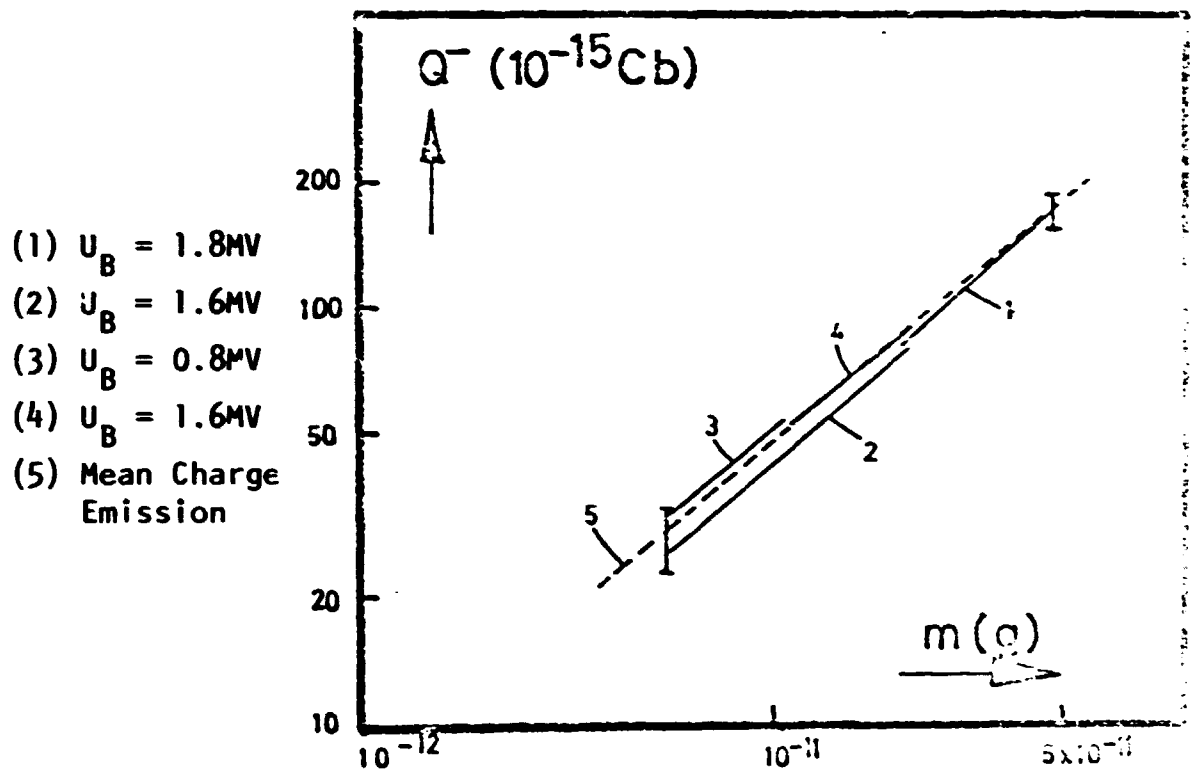

Figure 4a. Comparison of the Mass Dependence of the Charge Emission Under Variable Acceleration Voltage and Fixed Velocity (v = (2.04 ± 0.05) km/sec).

In the following experiments, which shall be treated at greater length in section 3.5., another possibility was found to test the independence of the charge emission from the charge condition of the projectile. In this case the /9

primary charge on the particle was stripped from it before impact on the target by going though a thin metallized plastic foil. The particle parameters m and v were not significantly altered at this time. Figure 4b compares the ion emissions measured on the impact of charged and uncharged particles.

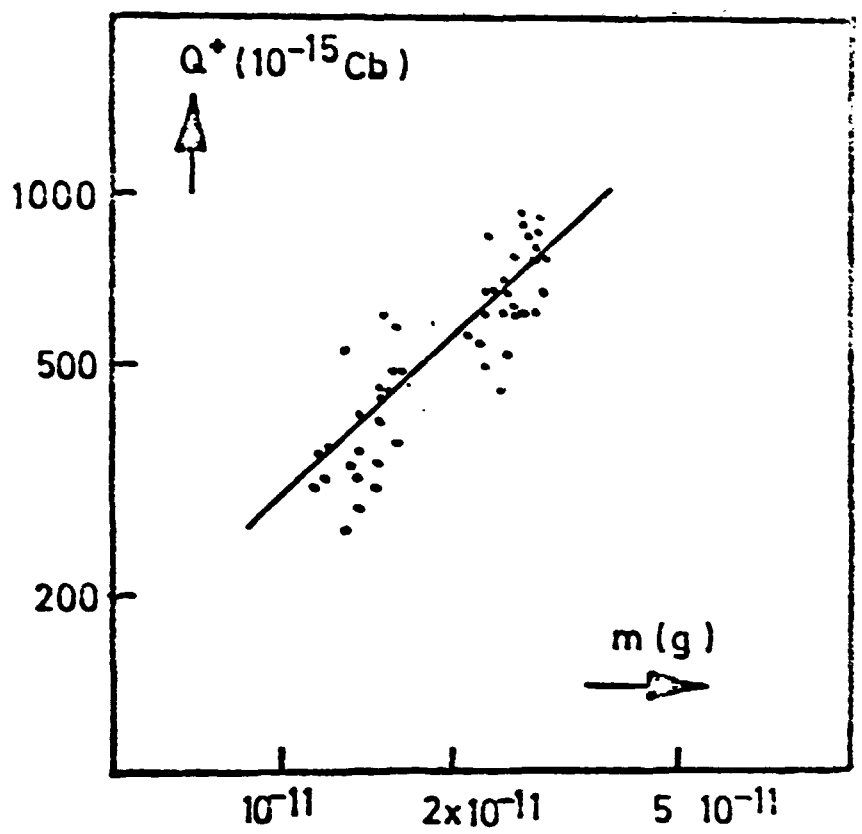

Figure 4b. Ion Emissions at the Impact of Charged and Uncharged Projectiles at a Constant Velocity (v = (5.25 ± 0.21) km/sec).

Plotted Line: Mean Value of the Charge Emission Upon the Incidence of Charged Particles;
Individual Measuring Points: Charge Emission for Uncharged Particles.

This diagram shows that the amount of charge liberated by impact in each case coincided well on the average. Only the distributions around the mean value can be seen as somewhat broader for particles which have passed through the foil. This is to be attributed to the fact that the mechanical parameters of the particles can still be upset to an insignificant degree in passing through the foil.

3.2. Influence of Charge-Separating Field on the Measurement of the Liberated Charge /10

Since at the time of particle impact about the same amounts of positive and negative charge carriers are liberated, they must first be separated by an electrical field. Only after this can an exact determination of the amount

of charge for either or both polarities be taken. It is enlightening to find that the shape and power of this field are both responsible for the height and shape of the signal, which is caused by a kind of charge on an electrically prestressed collecting electrode. In recording experiments for cosmic particles, this signal is the carrier of information on the physical parameters of the impacted particle. The charge-separating field is to be chosen in such a way that a connection as abrupt and unambiguous as possible is guaranteed between the particle parameters (m, v) and the resulting information signal. In addition the detector should have as great a sensitivity as possible. In order to create such optimum conditions for particle recording, the behavior of the following magnitudes must be considered:

a) Signal-noise relationship of the strike signal under constant entry parameters. This magnitude is a suitable measurement for the absolute height of the strike signal, because the static is essentially presupposed by the charge-sensitive preamplifier.
b) $\Delta Q/\bar{Q}$ under constant entry parameters. In this case ΔQ should represent the mean breadth of the statistical fluctuations around the mean value $\bar{Q}$ of the striked signal under many cases of the same sort. Similar dispersions occurred in all experiments and because of their magnitude could not be attributed to the static of the preamplifier.

In a series of tests different experimental conditions were assumed in the area of the impact spot. The intention here was to find those conditions under which the information provided by the detector signal most easily reflected the actual entry parameter of the particle. The behavior of the above mentioned magnitudes provides a criterion for this. The related conditions can/11 be divided into two groups. In one case only the amount of charge was determined for one polarity; in the other case an attempt was made to measure the amount of both kinds of charge occurring for one individual case. A choice of the pertinent test arrangements is represented in Figure 5.

The charge emissions, normalized for the incident mass, (depending on velocity v) and the relative distributions of this magnitude for the different arrangements were compared. In those cases in which both kinds of charge were supposed to be obtained, the following shortcomings were found: in arrangement b.2. the charge separation of the plasma could only be obtained incompletely. In arrangement b.1. the larger amount of charge was always collected on the cylindrical electrode and on the opposing prestressed grid. Moreover the field in this arrangement proved to be unfavorable because a point occurs inside the cylinder with a vanishing field strength (degenerate point) which can lie in the vicinity of the impact point depending on the choice of the potentials of the collecting cylinder and the collecting grid.

Figure 6 shows cases for plane arrangements as represented in Figure 5a. /12 Along with the distance s between the target and collecting grid, the strength of the charge-separating field was also varied by the choice of the potential difference U between the target and the grid.

According to Figure 6 a detector geometry with a suitably large s appears as the most suitable for determining the amount of charge. The reason for this

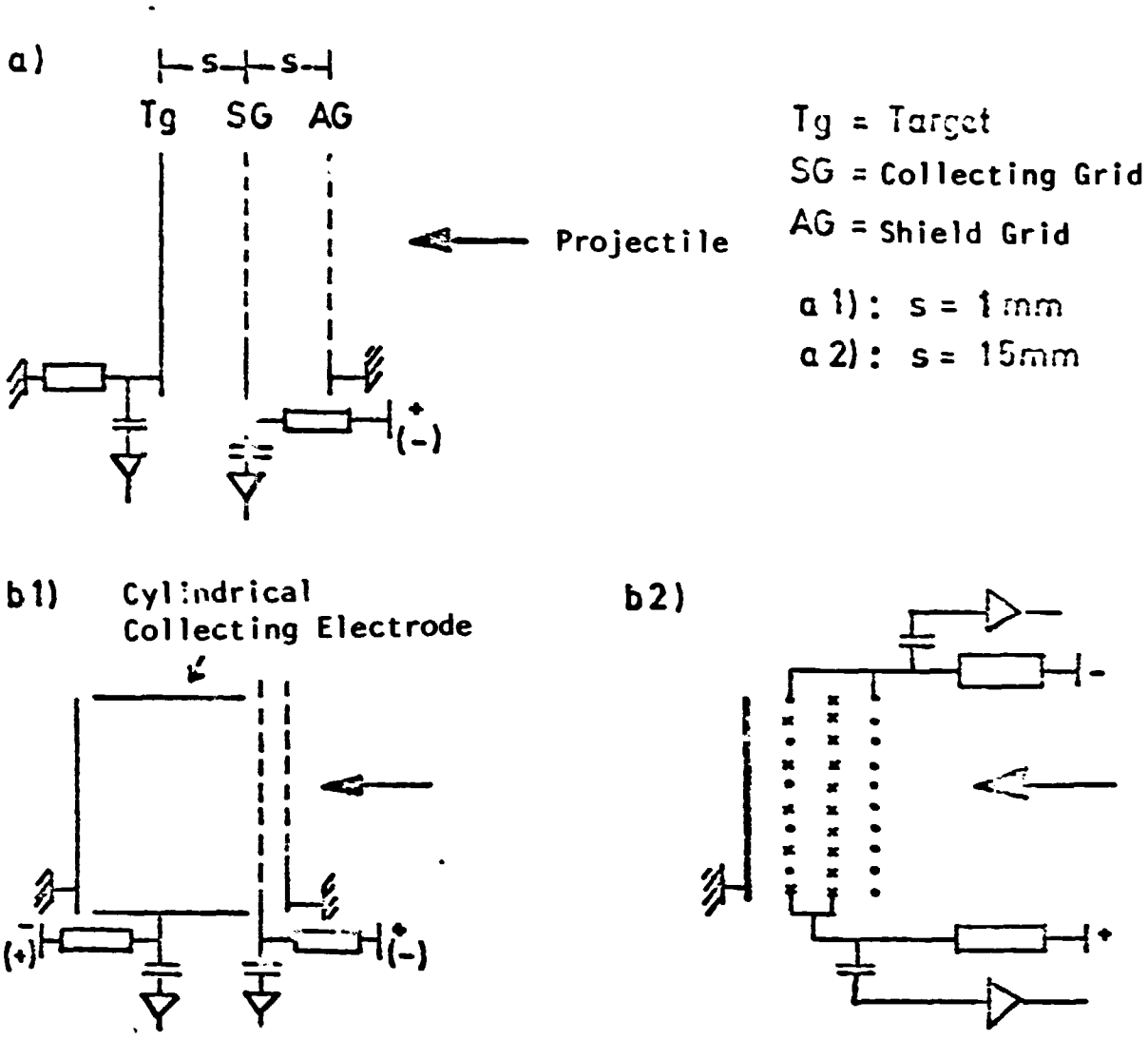

/11

Tg = Target
SG = Collecting Grid
AG = Shield Grid

a 1): s = 1 mm
a 2): s = 15mm

Figure 5. Arrangements for Measuring the Charge Emission on Particle Impact.

lies in the fact that the plasma can then expand in space for a longer period of time and thus be better separated from the field on the basis of the smaller density of charge carriers. This also explains why charge separation is obtained with smaller field strengths in greater distances s. /13

In section 3 6 it is shown that the amount of charge liberated upon impact depends upon the angle of incidence of the particle. Therefore it is to be assumed that the distributions of the charge emission originate to a certain degree from the unevenness of the target. Surface irregularities of the order of magnitude of the projectile dimensions are sufficient for this. Deviations of this type cannot even be removed by optimum detector geometry.

3.3. Dependence of Charge Emission on Mass and Velocity of Projectiles

The charge liberated by the impact of Fe particles was measured between velocities from about 0.9 km/sec up to almost 40 km/sec and with masses between

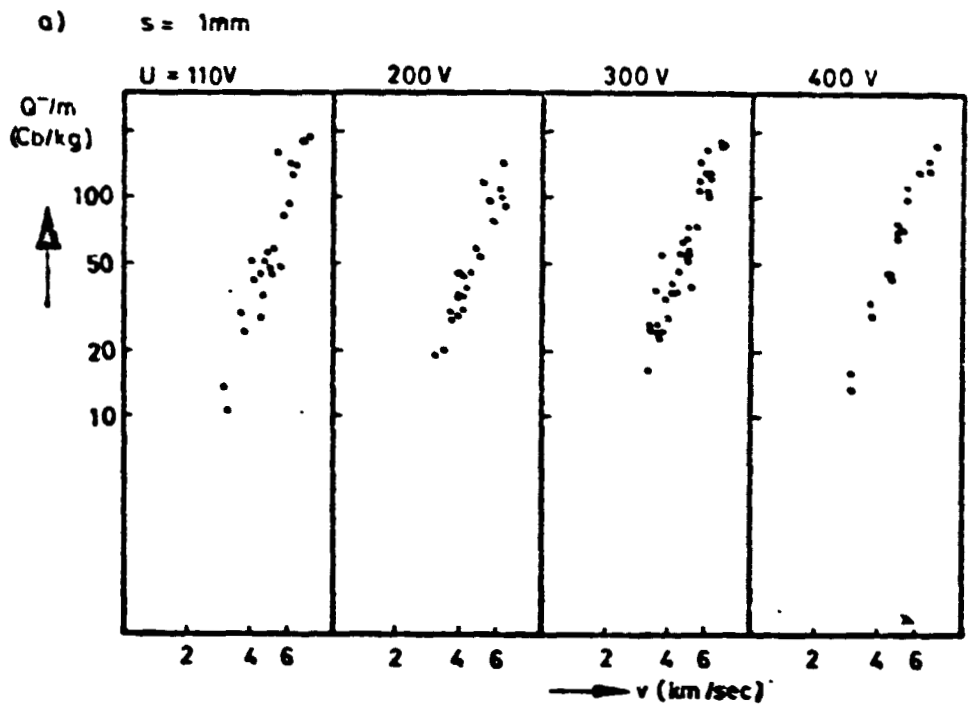

Figure 6. Q^-/m as a Function of the Velocity Under Various Test Conditions (Plane Detector System).

5×10^{-10} g and 10^{-15} g. For the reasons mentioned in 2.1. this entire range could not be covered by experiments to an identical degree. Thus it was particularly not possible to cover sufficiently broad ranges of mass with velocities over 8 km/sec in order to provide a statistical statement on the relationship between the charge liberated and the mass of the particles. Figure 7 shows cases of several experiments in which this statistical coverage was still

possible. The amount of charge liberated by impact was measured on a collecting grid with a distance from the target amounting to 10 mm with a potential difference of 40 V in respect to the target. This arrangement was always used below. A tungsten target was used as a collecting electrode.

/14

v = (4,03±0,13) km/sec

v = (5,14± 0,08) km/sec

v = (7,3± 0,2) km/sec

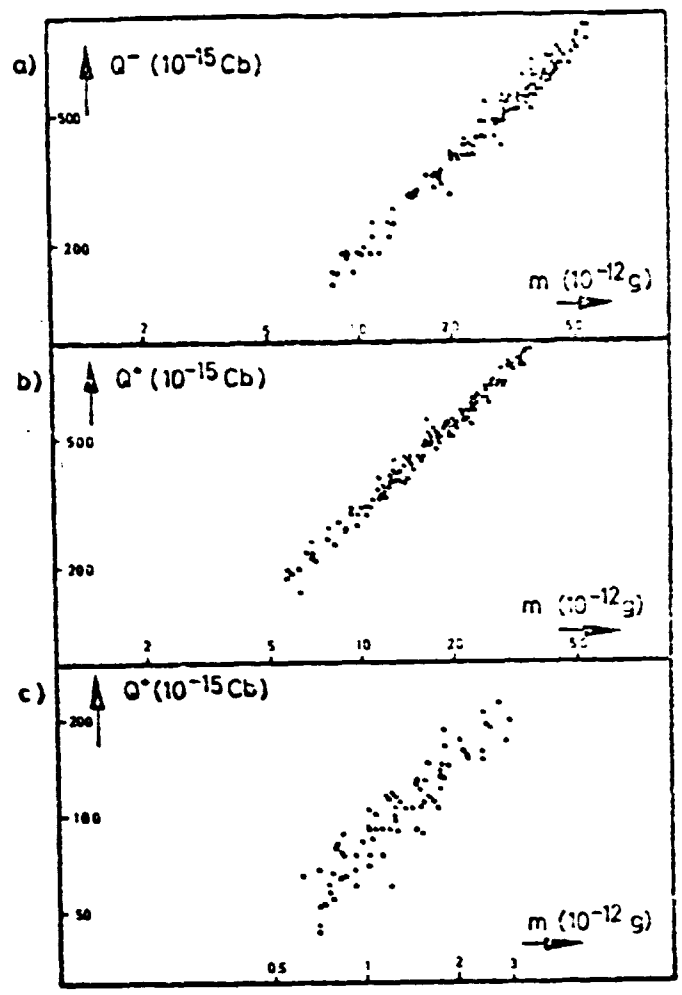

Figure 7. The Mass Dependency of the Charge Emission Under Fixed Velocities and Its Statistical Coverage From Individual Measuring Points.

In Figure 9 the charge emissions measured on impact are represented as a function of the mass under different, occasionally fixed projectile velocities. The diagram is completed by individual measuring points between 9 km/sec and 38 km/sec, which are available so far only from one photographed pace. Let us first explain the origin of these unusual measuring points by a few comments before we get to the matter of general conclusions which can be drawn from Figure 9.

The kinetic energy of a particle under a fixed acceleration voltage is proportional to its charge q and thus to the square of its radius r. Because the mass m is proportional to the third power of the radius, a proportionality

exists between the square of the velocity and the reciprocal of the particle radius. Thus rapid particles are small and therefore carry only a slight charge. If the projectile velocity comes into the order of magnitude of 12 to 15 km/sec, the charge on the particle can only be measured well if the static of the preamplifier on the cylinder detectors can be eliminated. For this purpose the transistor necessary for the first amplification stage was cooled to the temperature of liquid nitrogen. In spite of this such a charge measurement remained relatively inexact because the particle charge often shifted only a little above the static limit. The block diagram in Figure 8 shows in what way the time information on the particle flight through both analyzing detectors can be attributed to the particle filter. /15

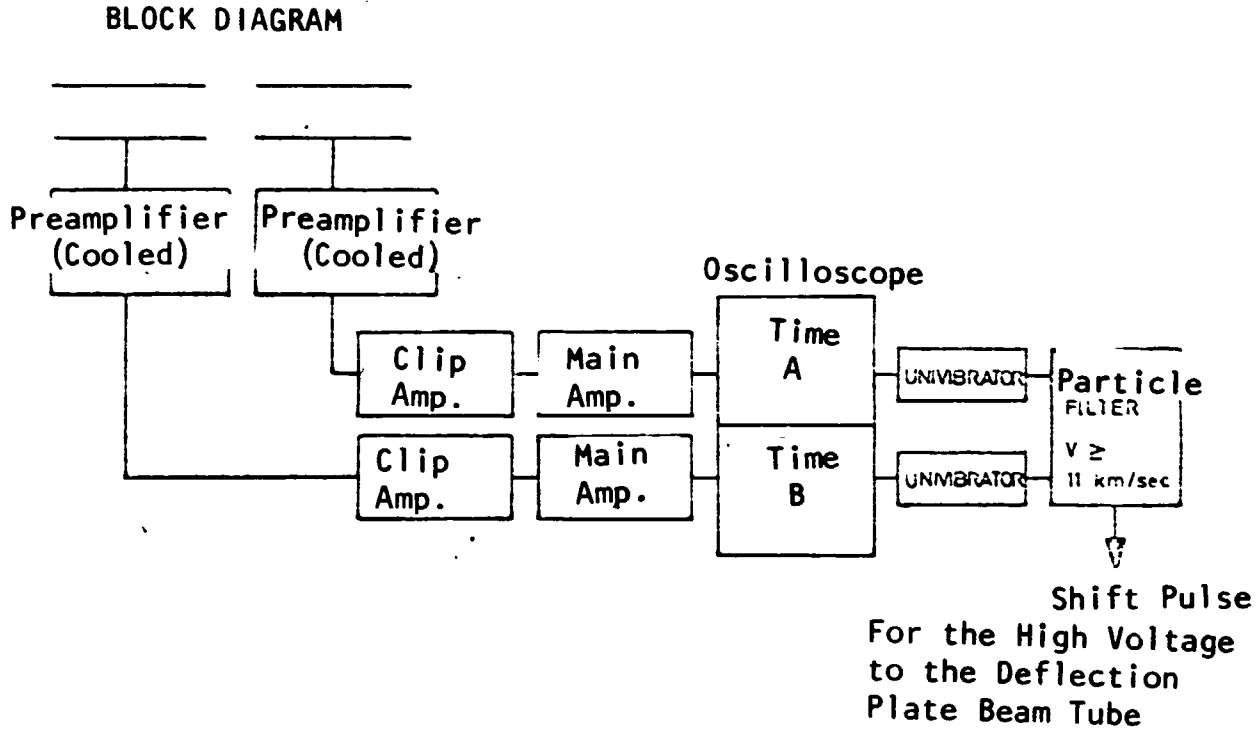

Figure 8. Processing of Detector Signal of High Speed Particle With Low Charge.

The oscillograph shown in Figure 8 had the following purpose. The signals which guided the saw to voltages for the time sweep of beams of A and B were referred to the particle filter as time markers. Since the detector signals show a characteristic form at the input A and B through the prearranged clip amplifier, even very small signals could be distinguished from static through fine regulation of the trigger thresholds. Thus only signals above the thresholds introduced could control the particle filter. This prevented random coincidences from static from putting the filter out of order. This measure was required because of the necessarily very high amplification of the detector signals. In normal operation it was not necessary. After separation another cylinder detector had to be flown through with a preamplifier which was also cooled. This is the one which measured the charge of the particle. Its velocity was provided by the travel time from entry into this detector

until impact against the target. /16

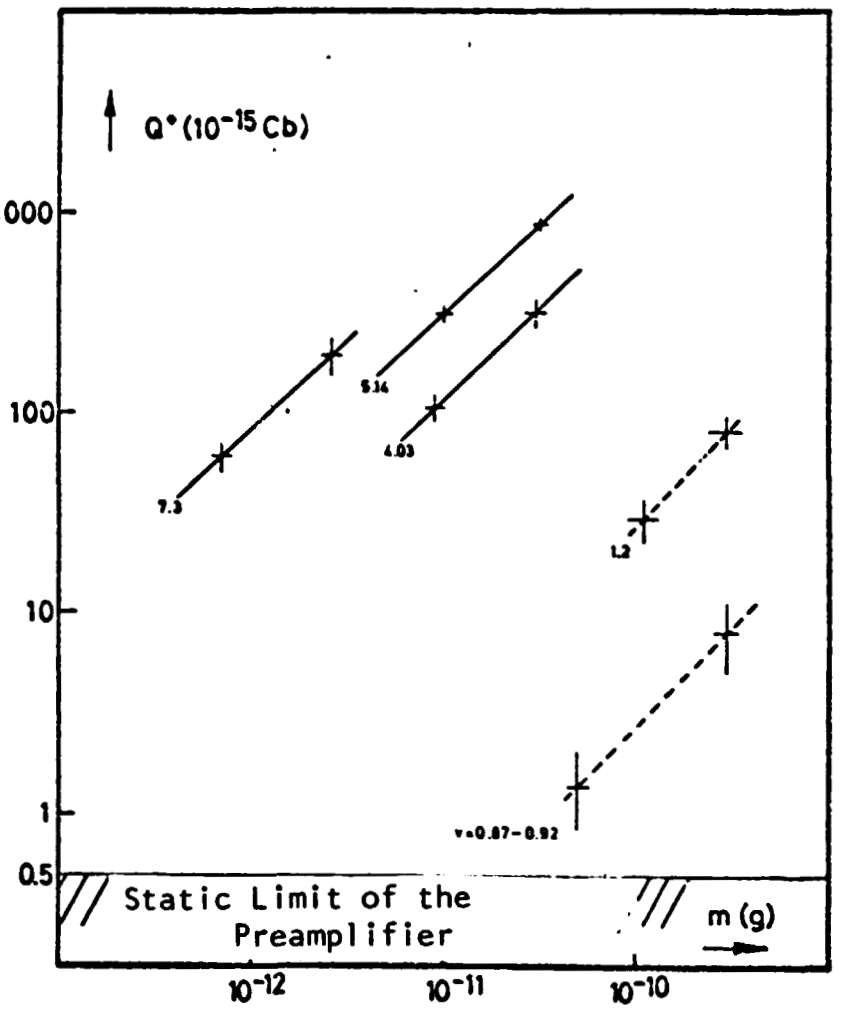

Figure 9. The Amount of Charge Liberated Upon Impact as a Function of the Mass Which has Entered.
a) Electrons
(See page 17)
b) Ions

Explanations for Figure 9: the error in mass measurement is given by

$$\Delta m / m = 2 \Delta v / v + \Delta q / q + \Delta U_B / U_B .$$

$\Delta U_B/U_B$ can be assumed as 0.01 and $\Delta q/q$ is determined by the accuracy of reading on the oscillograph (about 5%). In most cases v was determined exactly within two to three percent, which altogether causes a relative error $\Delta m/m$ of 10 to 12% for each individual mass measurement. Determination of the charge liberated is also affected by the accuracy of reading on the oscillograph with an error $\Delta Q/Q$ = 5%. As this charge approaches the static limit, the relative error increases. Groups of pairs of values ($m \pm \Delta m$, $Q \pm \Delta Q$) with v = constant are summarized by curves in Figure 9. Here the solid lines are the results of /17

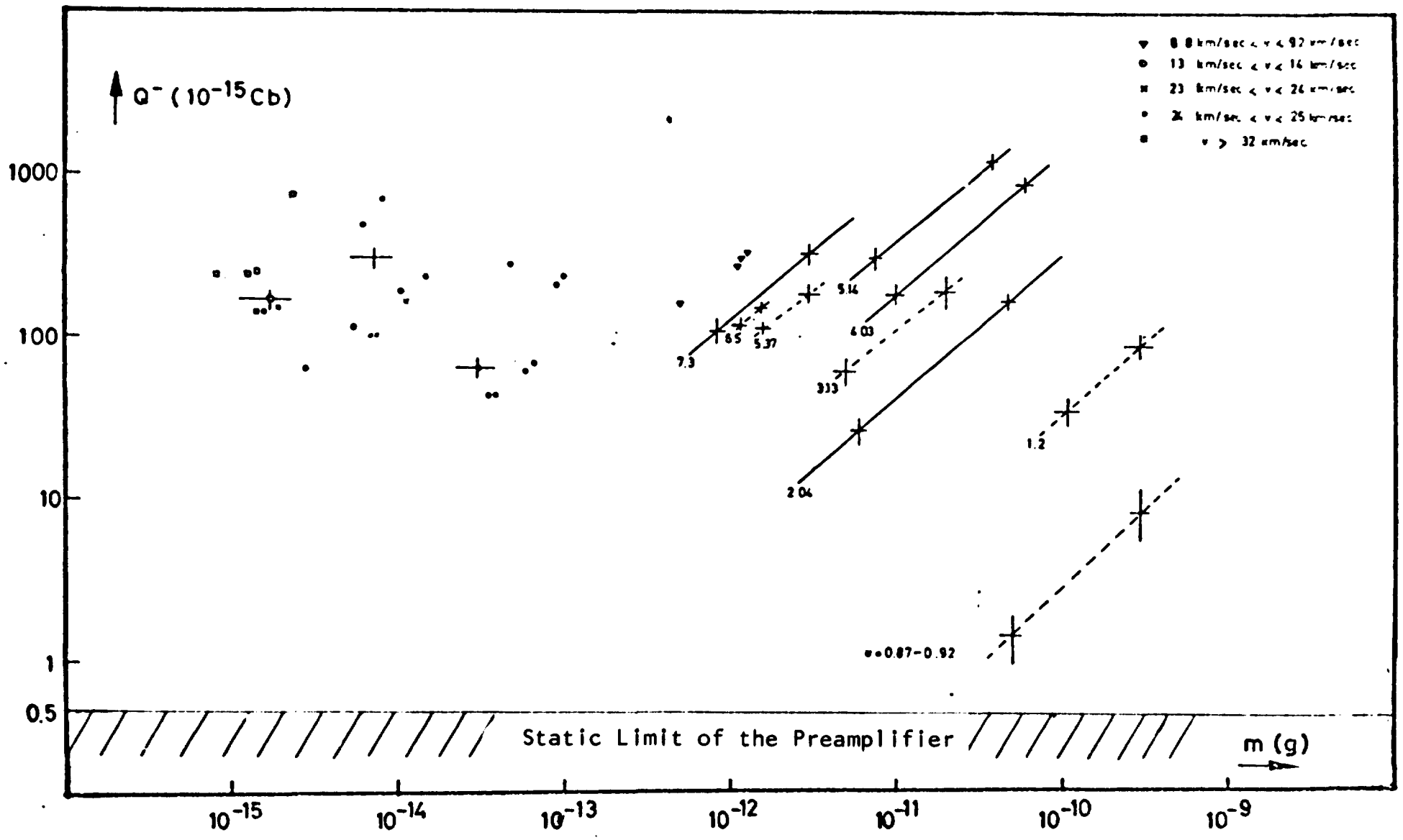

Figure 9a. The Amount of Electrons Liberated By Impact as a Function of the Mass Which Has Entered.

/16a

more than 70 individual measurements, and the broken lines from less than 30.

The rises of the straight lines in Figure 9 provide a mass exponent α, for which the relationship $Q \sim m^{\alpha}$ (at fixed velocity) is valid. In Table 1 the mass exponents valid for different velocities are provided.

Table 1. Mass Exponent α of the Amount of Charge Liberated at Different Particle Velocities.

v (km/sec)	α(El)	α(I)
0,9	1,0	1,0
1,2	1,0	1,0
2,0	0,9 $\pm$ 0,12	-
4,03	0,9 $\pm$ 0,12	0,91 $\pm$ 0,15
5,14	0,86 $\pm$ 0,15	0,9 $\pm$ 0,15
7,3	0,85 $\pm$ 0,17	0,89 $\pm$ 0,2

At higher velocities a light decrease in the mass exponents α is found. This phenomenon, however, can only be explained more thoroughly if the accessible range of mass for higher velocities is broadened. However, for an increase in v this becomes more and more difficult.

Table 1 shows that the charge emission in the lower velocity range is proportional to the particle mass. Therefore a representation in which the amount of charge liberated for the mass which has entered is referred to the velocity of the projectile, is reasonable. From such a diagram a velocity exponent β can be ascertained which is defined by the relationship $Q \sim v^{\beta}$ (at constant mass). Figure 10a shows representations of this type for electron and ion emissions. /18

Through the quotients

$$\frac{N(I)}{N(P)} = \frac{\text{Number of Ionized Atoms}}{\text{Number of Atoms of the Incident Projectile}}$$

an ionization activity cross section for the particle impact is given, which can be directly computed from Q/m. In Figure 10a a computation is made for this fact though an additional measurement for N(I)/N(P). This relationship is vanishingly small for low projectile velocities and only reaches the order of magnitude of 1% at v = 20 km/sec. In the velocity range 30 km/sec < v < 40 km/sec values between 5% and 20% already occur. /19

According to Table 1 the mass exponent at velocities over 2 km/sec amount closer to 0.9 than to 1. In order to obtain a reasonable velocity exponent β

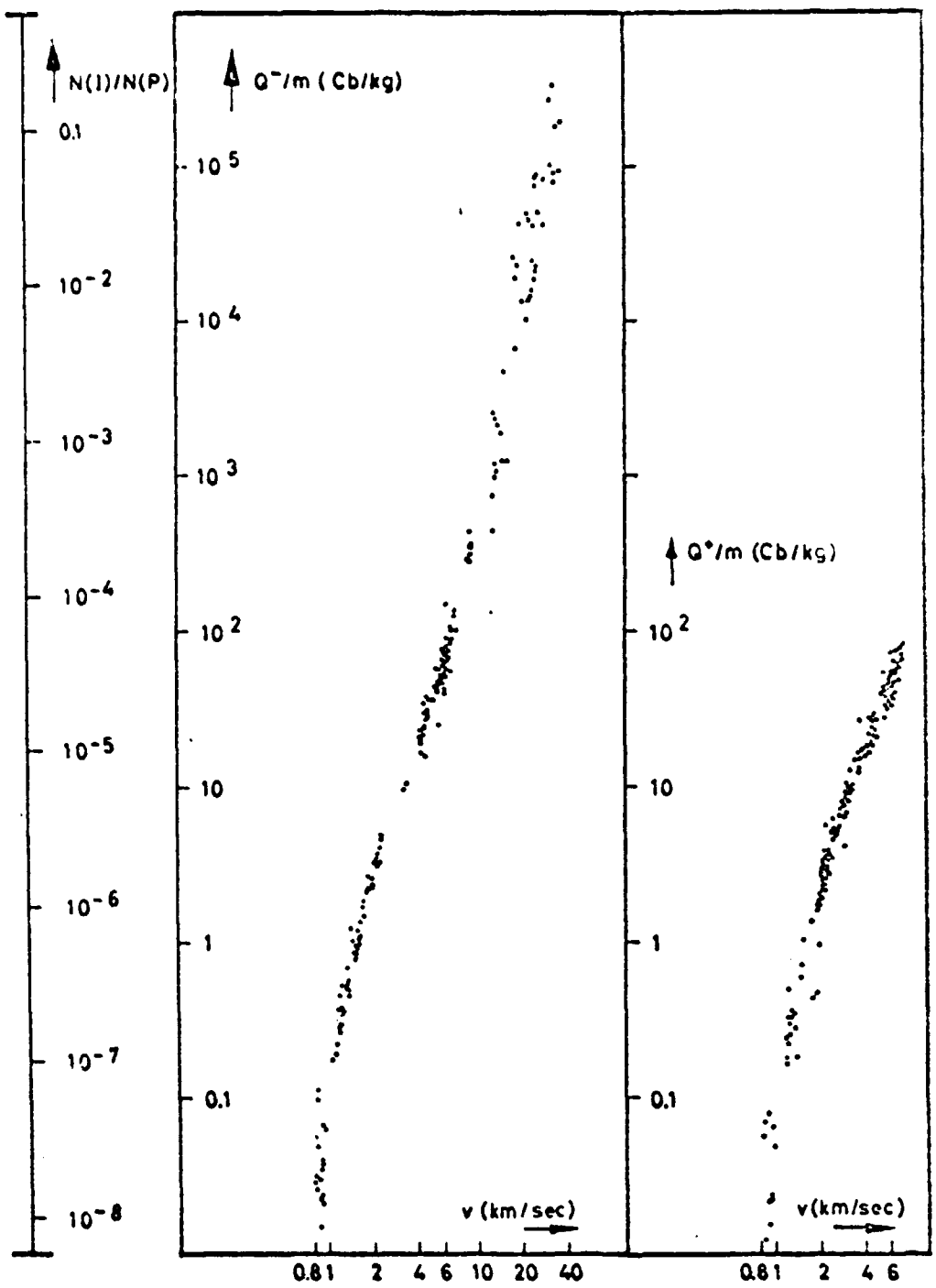

Figure 10a. Dependence of the Quotients Q/m on Velocity.

in this range also, the relationship between v and $Q/m^{0.9}$ will be considered.

After studying Figures 9 and 10, an all-embracing statement on the dependence of charge emission on the parameters m and v of the projectile is possible. For this three different areas of validity are chosen for best results: /20

a) $v < 2$ km/sec
b) 2 km/sec $< v <$ 9 km/sec
c) $v >$ 9 km/sec

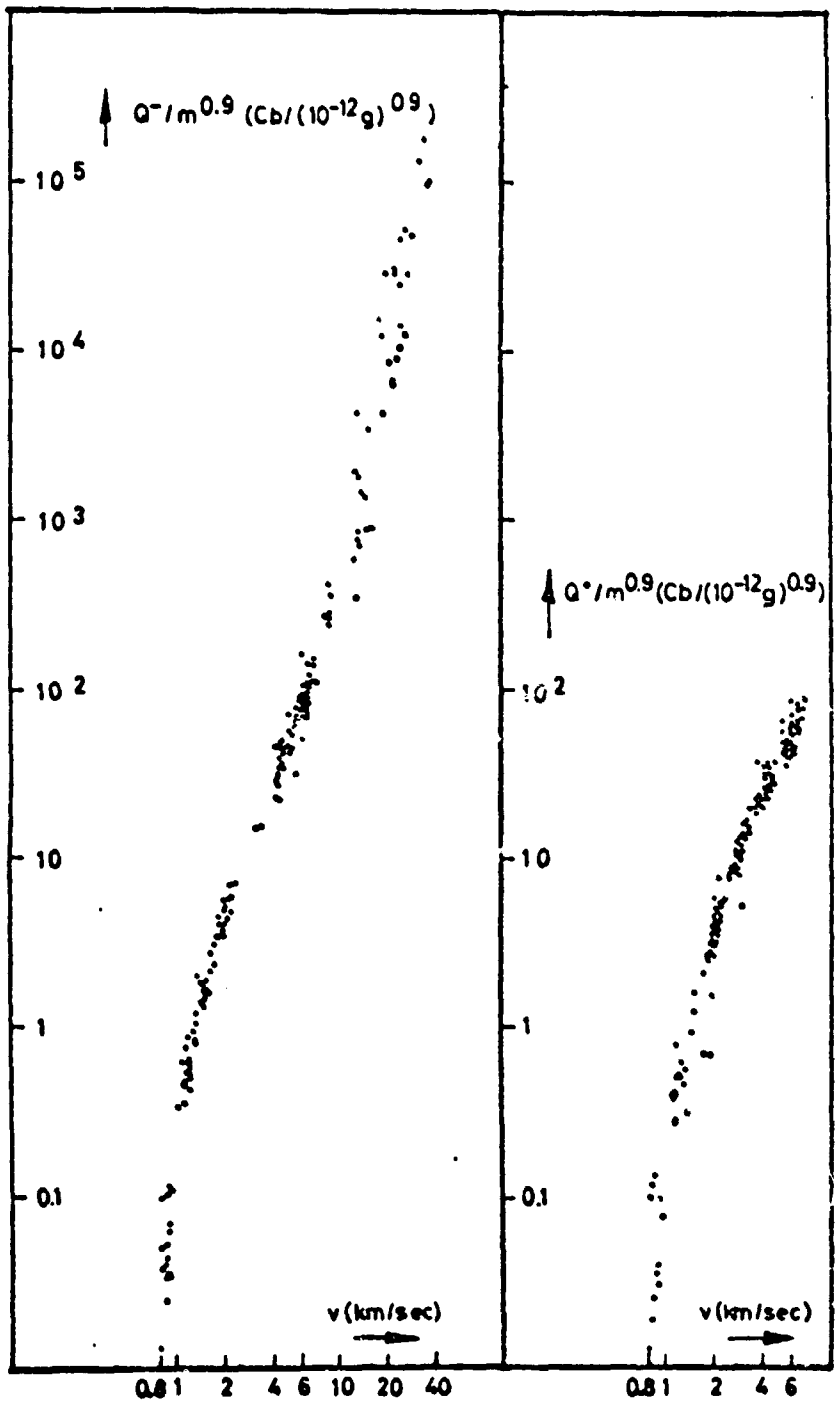

Figure 10b. Dependence of the Quotients $Q/m^{0.9}$ on Velocity.

a) Both Q^+ and Q^- can be considered at constant velocity v as magnitudes proportional to particle mass m. However, no more exact velocity exponent β, generally valid for this range, can be provided. This is because, as can be seen from Figure 10a, $\frac{\log (Q/m)}{\log v}$ is not constant. β is itself rather a function of v with the properties

$$\beta \; (\; v=2\text{km/sec} \;) \simeq 3$$
$$\beta \; (\; v=0,9\text{km/sec} \;) \simeq 7 - 8$$

The curves $Q/m = Q_{normalized} = g(v)$ thus descend more and more abruptly in the logarithmic representation of Figure 10a, when v approaches from above the position v = 0.8 km/sec. This means that in the vicinity of this position ther exists a limiting velocity. Below this limiting velocity the effect of the formation of free charge carriers when microparticles strike is vanishingly small. The fact that in the vicinity of the position v = 0.8 km/sec for the function log ($Q_{normalized}$) a perpendicular tangent can be presumed to serve as a basis. This statement is corroborated by the fact that in the area 0.87 km/sec < v < 0.92 km/s, the charge emission has already sunk for about 30% of all cases considered below the static limit of the preamplifier.

b) In the area 2 km/sec < v < 9 km/sec, a complete analytic relationship between the charge emission and the entry parameters can be provided, and it will describe the measuring results available within the limits of error. For both charge polarities it reads:

$$(I)\quad Q^- = const_1\ m^{\alpha_1}\ v^{\beta_1} \quad \text{with} \quad const_1 = 0{,}54 \pm 0{,}03,\ \alpha_1 = 0{,}9 \pm 0{,}15,\ \beta_1 = 2{,}8 \pm 0{,}3$$

$$(II)\quad Q^+ = const_2\ m^{\alpha_2}\ v^{\beta_2} \quad \text{with} \quad const_2 = 0{,}49 \pm 0{,}07,\ \alpha_2 = 0{,}9 \pm 0{,}15,\ \beta_2 = 2{,}7 \pm 0{,}4 \qquad /21$$

In these empirical equations, m is to be introduced into many cases of 10^{-12} g and v in km/sec, in order to obtain Q^- or Q^+ in the unit 10^{-15} Coulombs.

The determination of α_i, β_i and $const_i$ occurred in the following way:
α_i from Table 1.
β_i by approximating the measuring points in Figure 10b through a straight line, the ascent of which provided β (as a result of the doubled logarithmic scale).
$const_i$ by introducing triple values (m, v, $Q^{\pm}$).

c) In this velocity range the explicit assertion of a functional relationship between the charge emission and the mechanical parameters of the projectile are waived for the following reasons:

1) the mass determination for projectiles with v > 10 km/sec was made more difficult because the charge of these particles, as mentioned above, sometimes lay only slightly above the static limit of the analyzing detectors.

This is a reason for the considerably greater distribution of measurement results in this range.

2) At these velocities no systematic investigation of the dependence of the amount of charge liberated on the mass could be carried out, because the masses occurring for constant velocity were not sufficiently dispersed and because such fast particles are naturally quite rare.

However, it is clearly recognized in Figure 10 that the behavior above 10 km/sec in a reasonable way confirms the measurements which were obtained at lower velocities. It was found that at high projectile velocities the good sensitivity to mass expected is found. One example: at v + 30 km/sec or more, a particle of 10^{-15} g releases a charge of not less than 10^{-13} Coulombs. This allows us to expect that with similar projectile velocities and with a charge indication limit of 10^{-16} Coulombs, particles of the order of magnitude of 10^{-18} g can still provide a useful detector signal. (Mass proportionality is assumed as a first approximation for this extrapolation.)

3.4. Influence of Target Properties on Charge Emission /22

According to [9], tungsten is a suitable material for serving as a target in a plasma detector to record cosmic particles. The probability existed that the charge productivity of a target was related to its degree of impurity in alkalis and earth alkalis. This reflection goes back to the following model representation: upon particle impact a momentaneous condition of high energy density is produced at the point of impact and this condition brings a certain part of the target or particle material into a state of vaporization. A relatively high alkali content in this resultant cloud of vapor increases the number of the charge carriers liberated in it, because the ionization work of the alkalis is small in proportion to that of other components of the vapor which are present.

Therefore tungsten targets, which were produced or pretreated in different ways (e.g. by different kinds of annealing), were shot with identical particles and their charge productivity was compared. The potassium and calcium content of these targets was ascertained with the help of an x-ray fluorescent analysis. According to this all of the targets used had about the same degree of impurity; the potassium or calcium content amounted from 0.5 to 1 per thousand. The assumption is possible that in annealing only the impurity components directly adsorbed on the surface could be dislodged, while an x-ray fluorescent analysis of the impurity contents was performed in a deeper layer.

Table 2 shows the charge emission for the different targets under identical entry conditions. The result of this is that the same degree of charge productivity cannot be assigned to every tungsten target. For a specific target surface used in a flight experiment, therefore, the determination of its characteristic properties by standard experiments is necessary.

3.5. Measurement of Charge Liberated at Target Impact After a Previous Passage of the Particle Through Special Plastic Foils /23

Table 2. The Charge Productivity of Different Tungsten Targets Under Fixed Entry Conditions.

$v = 5{,}14 \pm 0{,}08$ km/sec ; $m = (2 \pm 0{,}2) \times 10^{-11}$ g

Kind of Target	Charge Emission (10^{-15} Cb)	
	Q^+	Q^-
Untreated Tg., 100 μ Thick	716 ± 56	770 ± 50
Highly Polished Tg., 1 mm Thick	548 ± 48	693 ± 40
W-Schicht, 14 μ Thick (Deposited by Cathode Sputtering)	604 ± 96	694 ± 108
Tg. Annealed in Atmosphere	592 ± 94	798 ± 92
Tg. Annealed in a High Vacuum	562 ± 36	766 ± 51

Experiments to determine the flow of cosmic particles incident to the earth usually take place in the ionosphere. In recording individual particles with a plasma detector one is advised to shield target surfaces and grids against the external plasma. Such shielding can be achieved by a metallized plastic foil. If the volume of the detector shut out by the foil can still be further from off, it would be possible at lower levels to take measurements in which the external pressure hinders a satisfactory rapid expansion and collection of the charge liberated. A foil used as a shield should still be penetrable for particles with velocities of 1 km/sec, because the relative velocity between particles and detector in flight experiments can lie in this order of magnitude. The parameters m and v of the incident particles should be prejudiced as little as possible by these foils.

Various foils were tested with iron projectiles for their usefulness as shielding. For this the velocity of the projectiles was determined before and after passage through the foil and the charge still liberated after particle impact was measured. Figure 11 provides information on the measuring methods used for this. /24

The peculiar signal shape presented in Figure 11b comes into being at the exit of the preamplifier 1 (see Figure 11a) as follows. At time t_1 the positively charged particle comes through the grid G1 and there influences a maximum charge of the opposite sign. The influencial activity on G1 continues to decline until time t_2 because the field of the particle charge is shielded more and more from the grounded grid G2. After passing G2, the influential activity

a) Test Arrangement

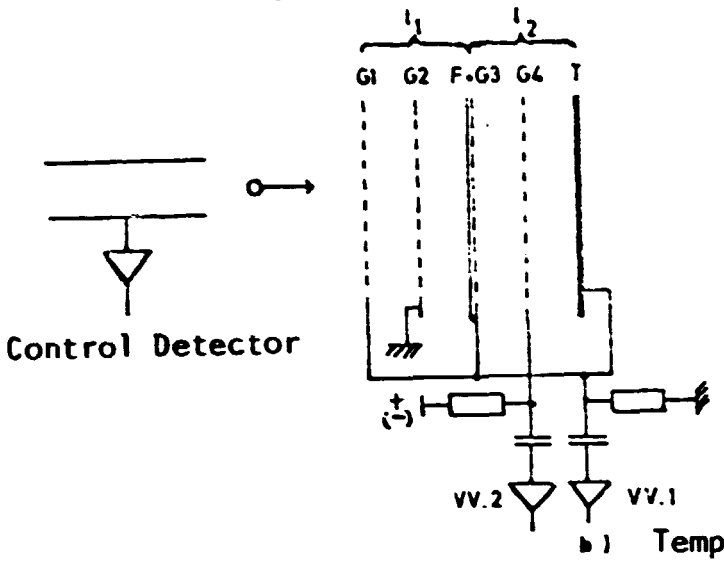

b) Temporal Signal Course at Preamplifier

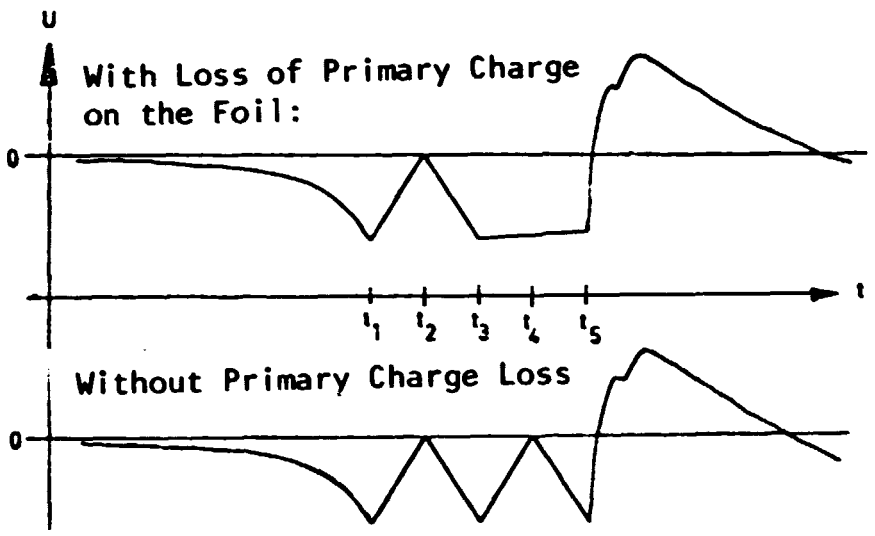

Figure 11. Experiment to Investigate the Charge Emission After a Particle is Previously Passed Through a Foil.

increases on G3 until time t_3. The shape of the signal for time $t > t_3$ now indicates whether the original charge of the particle, and how much of it, still remains or has been removed by the foil which is spread over G3. Finally, at time point t_5, impact is made on the target. Both of these periods of time $(t_3 - t_1)$ and $(t_5 - t_3)$ make it possible to ascertain the velocity of the particle before and after going through the foil when the geometrical dimensions of the arrangement are known. /25

According to the method described above, several foils were investigated with reference to their activity on the mechanical parameters m and v and thus on the charge emission upon impact. The foils used were:

a) a 2μ thick hostaphane foil;
b) a 500 Å thick nitrocellulous foil;
c) a nitrocellulous foil, 0.2 to 0.4 μ thick, with Al deposited as a vapor. This foil on a support grid always resists a pressure difference of over 100 Torr. on both sides of the foil.

Foils b) and c) were produced by dropping a nitrocellulous solution of known concentration onto a pure water surface where it is spread out in a thin layer and dried. The thickness of such foils could be estimated from the weight of one drop, the extended surface, the concentration of the solution and the density of the nitrocellulous.

In Figure 12 the charge emissions normalized for mass unit, which were still liberated upon impact after the particles had gone through the different foils, are plotted for velocities v_1 and v_2 before and after going through the foils.

/26

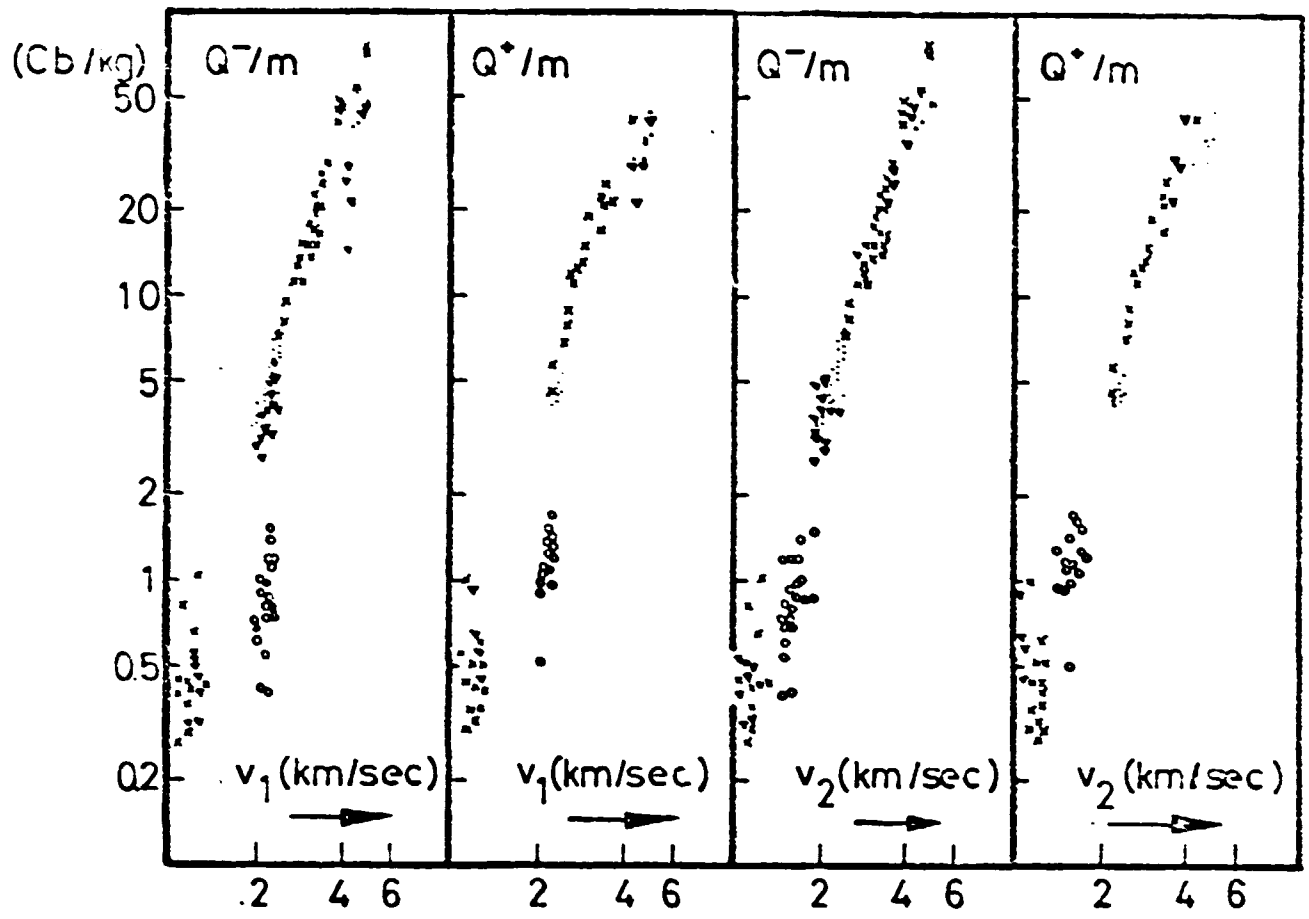

Figure 12. Q/m as a Function of Velocities v_1 and v_2

v_1 = Velocity of the Projectile Before Going Through the Foil

v_2 = Velocity of the Projectile After Going Through the Foil

o is the 2μ Thick Hostaphane Foil

▽ is the Nitrocellulous Foil, 0.2 to 0.4 μ Thick, With Al Deposited as a Vapor

x is the 500 Å Thick Nitrocellulous Foil

• is Bombardment Without Foils

According to the experiments carried out, the following judgments can be given on the properties of the individual foils examined:

a) After going through the 2μ thick hostaphane foil, a considerable

deviation for v_1 = 2 km/sec could be determined between the charge emission actually released and that to be expected in bombardment without foils. This deviation is explained by the braking of the particles in going through the foil and therefore disappears for the most part if the charge emission normalized for an incident mass is referred to v_2. Particles with v_1 = 4.1-4.8 km/sec could not be picked up any more beyond this foil. Because of the choice /27 which the accelerator makes, these particles are naturally smaller than those with v_1 = 2 km/sec. Validities for this experiment were: particle diameter D: 0.6 μ < D < 1.1μ at v_1 = 2 km/sec; 0.2μ < D < 0.3μ at v_1 = 4 km/sec. Therefore such small particles do not penetrate this foil any further. At velocities v_1 = 1.0-1.2 km/sec the impact of the particles could not be observed on the target any more if the foil covered it. This means that these particles, even if they have penetrated the foil because of their magnitude, were still braked to a velocity which lay below the limiting velocity mentioned in 3.3.

After evaluation of this condition, it can be said that this foil is not suitable for use in a plasma detector.

b) The 500 Å thick nitrocellulous foil does not have any effect on the mechanical parameters of the particle in the range investigated (v_1 = 1.0-4.8 km/sec). The same is true of the amount of charge liberated by impact on the target in contrast to those with bombardment without foils. The slight mechanical resistance of this foil, however, also makes it useless as a shield.

c) Passage through the metallized nitrocellulous foil 0.2 through 0.4μ thick establishes the fact that the particle really does lose its charge, but that the amount of charge liberated at target impact is not essentially diminished in contrast to bombardment without foils. A slight reduction in charge emission could be noticed only at v_1 = 4.1-4.8 km/sec. The particle diameter D in these cases amounted to 0.2 to 0.4μ. Foil c) is a compromise between the two extreme cases a) and b). With only a slight braking effect, it offers the advantage of a definite mechanical capacitance. Under the given conditions foils with similar properties seem to be the best suited for keeping an external plasma in residue from the target surface and grid of a plasma detector.

These determinations were made with Fe particles. For projectile material of a lesser density it is to be presumed that the foils investigated here would cause more braking. This would have the result that a plasma detector equipped with shielding foils would be the more sensitive in the flight experiment, the lower the density of the particles to be expected is.

3.6. Dependence of Charge Emission on Angle of Incidence of Particle /28

For the recording experiments the plan is to use the information on the amount of charge liberated by a particle impact to express the mechanical parameters of the particle which has caused such an event. Thus the particle mass could be approximately ascertained for the known detector calibration

$Q = \text{const } m^{\alpha}v^{\beta}$ by evaluating the relative velocity between detector and particle. However, the velocity and liberated charge under such a condition are still not able to settle the incident mass unambiguously. For, a dependence of this charge on the angle of incidence Θ of the projectile is shown. The connection between the charge carrier emission and this angle was investigated for several targets. It was first detected on a molybdenum target which has a very obvious angular behavior.

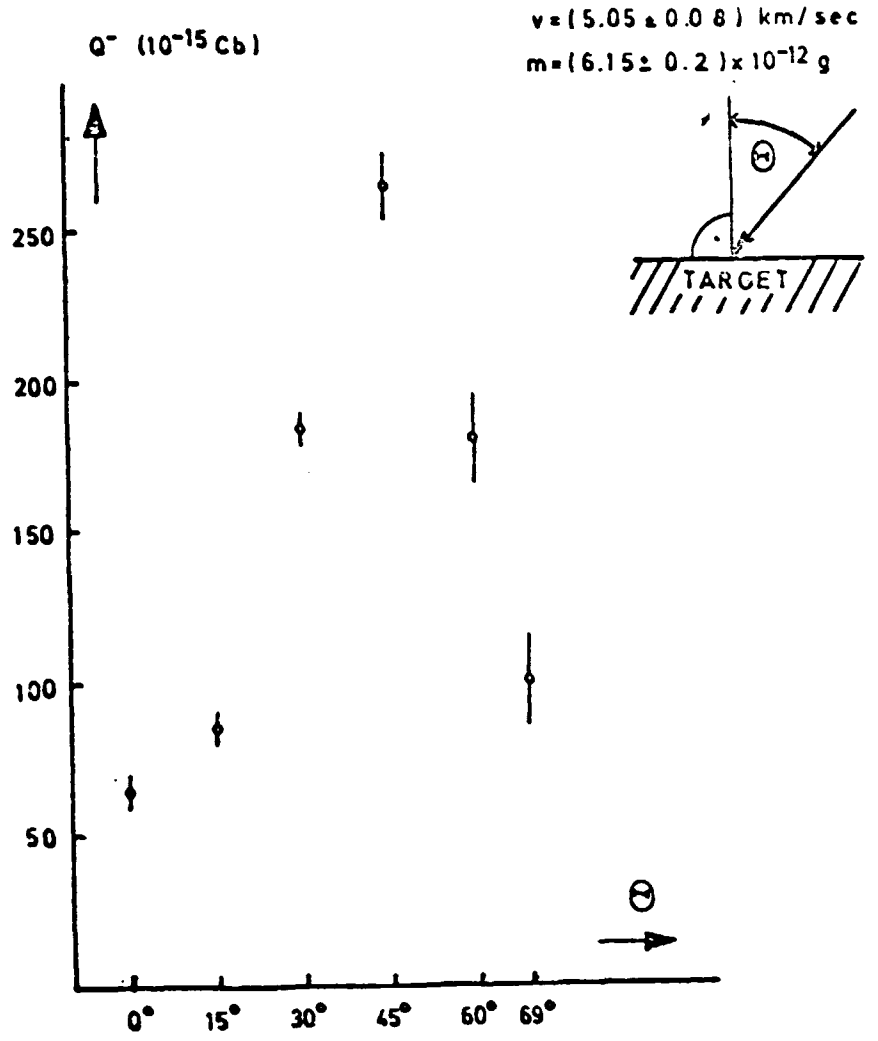

A maximum charge emission, increased by a factor of 4 over the perpendicular incidence, is found at about 45°.

Figure 13a. The Angle Dependence of the Charge Emission for a Molybdenum Target.

In Figure 13b the charge liberated upon impact with projectile velocities of 4, 5, and 6 km/sec is compared as a function of particle mass for both cases $\Theta = 0°$ and $\Theta = 45°$. Molybdenum was used as a target material. /29

It turns out that at fixed velocity the ratio $Q(\Theta)/Q(0°)$ is independent of mass and is only a function $f_1(\Theta)$ of the angle of incidence. Likewise with a fixed mass $f_2(\Theta) = Q(\Theta)/Q(0°)$, it is independent of velocity in the range under investigation and $f_1(\Theta) = f_2(\Theta)$ is valid. A

plasma detector which shows such an angular behavior can be characterized by a calibration equation of the following simple form:

$$Q = \text{const}\ f(\Theta)\ \ m^{\alpha}\ (v_{rel})^{\beta}\ ;\quad f \quad \text{independent of} \quad (\ m\ ,\ v\ )$$

Therefore Q can be represented as the product of three functions in which only one entry magnitude occurs.

The behavior of two different tungsten targets is represented in Figures 14a and 14b. A smaller value for the quotients $Q_{maximal}/Q_{perpendicular}$ turns up as an essential difference from molybdenum.

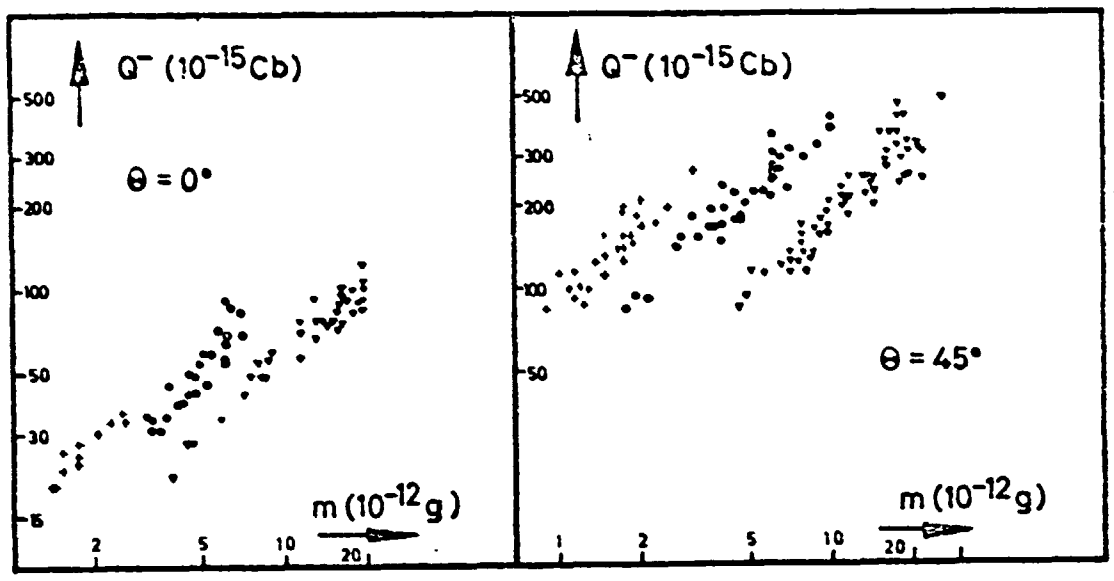

Figure 13b. + v - (6 ± 0.1) km/sec
o v = (5.05 ± 0.08) km/sec
∇ v = (4 ± 0.2) km/sec

Here let us try to give a simple meaning to the oblique incidence of particles in harmony with the proper behavior of the function f(Θ). For this purpose we first wish to proceed from the following assumptions: /30

1) The kinetic energy of the particle is transferred at the place of impact and is, for the most part, at the moment of impact concentrated on a narrow spatial area of the order of magnitude of the particle volume. This assumption is founded on the fact that energy transportation away from the place of impact cannot be carried out in a sufficiently short time, particularly if the particle insides with ultrasonic velocity relative to the target material. As a result of this high energy density, the neighborhood of the impact point is heated and can lead to the melting and evaporation of projectile or target material. Let us designate the space where this is possible as "excited volume."

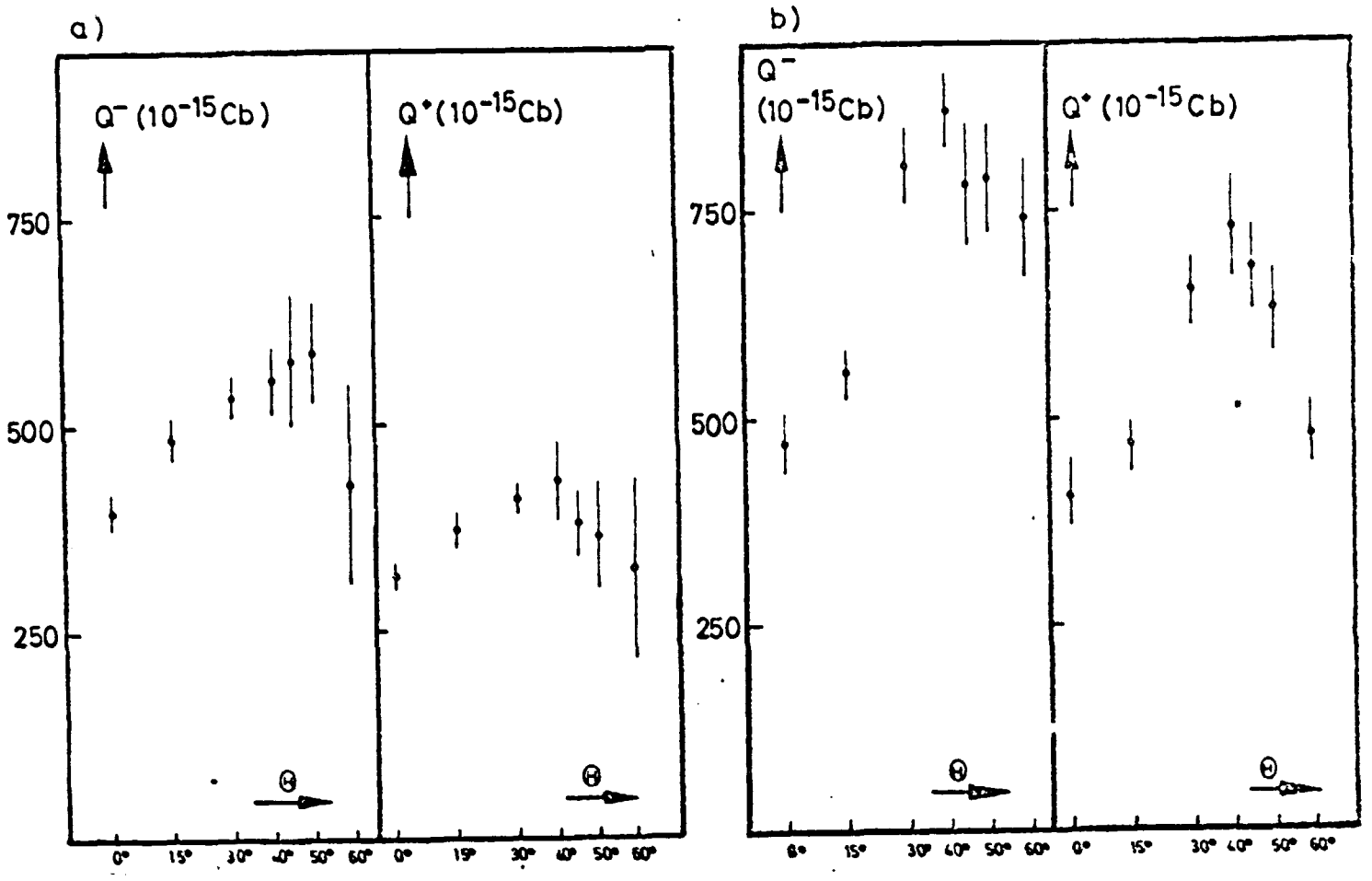

Figure 14. Dependence of the Amount of Charge Liberated on the Angle of Incidence Θ of the Particle When the Other Mechanical Entry Parameters are Held Constant.

$v = (5.25 \pm 0.21)$ km/sec

$m = (13.6 \pm 1.1) \times 10^{-12}$g

a) Highly Polished Tungsten Target.

b) Tungsten Layer, 14μ Thick (by Cathode Sputtering on Al).

2) The number of charge carriers liberated on the occasion of particle impact will depend on the "free surface" of the excited volume. Let the free surface be that part of the area of contact of the excited volume on which this volume is not limited by solid material. /31

3) The free surface of the excited volume is increased when the particle fall obliquely. This assumption seems enlightening if the velocity vector of the particle is split into tangential and normal components with respect to the target surface. While the normal component determines the penetration depth and thus the depth of the excited volume, the tangential component expands the excited volume on the target surface. In this way there is an increase of the surface on which free charge carriers and material to be vaporized can hit.

These three assumptions give an explanation of why the charge liberated

on impact under oblique conditions should first increase with angle Θ. Other reasons also illustrate the fact that after going through a maximum the charge sinks again with a sufficiently flat particle incidence.

4) With a flat incidence the particle can be reflected on the target surface. The following reflections lead to this conclusion. As a result of the small normal component of the particle impulse with very flat angles of incidence, only a slight penetration depth can be reached (perhaps only a fragment of the particle diameter). Then on the basis of this almost completely superficial contact, the very great tangential impulse cannot be exchanged between projectile and target, or be taken up by the target. This condition causes a reflection or at least a further movement of the particle in the direction of the tangential component of its initial impulse. Such a particle naturally takes a considerable part of its kinetic energy away with it. The angle of incidence thus also determines whether the shot between particle and target takes place in a completely inelastic manner or not.

5) With an oblique particle descent, especially in the angular range in which the tangential component becomes larger than the normal component, it can be figured that the incident energy is distributed to a larger and larger volume because of the altered entry conditions. This is also noticeable in a drop of the energy density on the free surface. This can again have the result that /32

a) less material is vaporized from the free surface,
b) the temperature of this emitted vapor is less than that produced by the same particle with a more perpendicular incidence,
c) the number of charge carriers occurring directly from solid material is lessened.

It is to be assumed that the total number of liberated charge carriers, which alone is capable of measurement, is composed of two particles of different origin. On the one hand these are the charges which come directly from the projectile or target material; they are predominantly electrons, because they do not have to overcome a grid bond as do metal ions. On the other hand, the vapor cloud emitted, which occurs partly ionized because of its high temperature, also provides an essential contribution to the total charge measured. In this portion ions and electrons are present in equal amounts. This explains the fact that the electron emission generally lay somewhat higher than the ion emission. However, it is also clear that all three effects a), b) and c) draw a lesser total liberated charge along with them.

It is to be assumed that reflections 4) and 5) can no longer be disregarded for certain angles. As a result of the experiment at least one of them from about 45° should be significant.

The dependence of the charge emission liberated on the angle of incidence of a particle leads to difficulties in carrying out a flight experiment. For evaluating such a test it is naturally desirable to possess information about the angle of incidence for each individual occurrence. Under certain suppositions this is possible for a rocket experiment, particularly if the rocket

velocity can be considered as larger than the specific velocity of the particle. In this case the angle of incidence of the particle is given by the angle between the deflection of the flight of the rocket and the perpendicular to the detector surface. When the particle velocity is comparable to or greater than the rocket velocity, it is no longer possible to simply ascertain /33 the angle of incidence. Then it is only limited by the detector geometry. This must first of all be interpreted on as high a rate of occurrence as possible, i.e. no angular range can be left out of consideration. However, for experiments in which the determination of the angle of incidence is critical, there might be found a target material which has a value $Q_{maximal}/Q_{perpendicular}$ as close to one as possible. In this way one would always be able to keep the error in determining the mechanical parameters of the particles found relatively small, even if the angle of incidence were unknown. A comparison of Figures 13a, 14a and 14b show that targets in this sense can have an individual angular behavior. Naturally in a flight experiment attention must also be given to the fact that the surface irregularities of the target are smaller than the dimensions of the particles expected. Even with a known direction of incidence, different striking angles might occur in microscopic subdivisions.

4. Discussion

This work did not have the primary purpose of explaining a physical process. The primary task consisted more in the creation of experimental findings which would make possible a substance-oriented execution of experiments in recording cosmic particles. Before going into the consequences resulting from the findings for the construction of such experimental recording collected in Chapter 3, let us first give a comprehensive phenomenological description and partial significance of the effect exploited here.

When high energy Fe particles impact against metallic targets, charges of both polarities are liberated in about equal parts. This allows the conclusion that this cannot only refer to a result of a purely thermal charge carrier emission from the metals. In such a case electron emission would be extremely predominant. Thus we can proceed from the fact that a considerable portion of /34 the charge carriers liberated come from a partially ionized vapor cloud which is formed when a particle strikes. On the average the number of negative carriers lies 10 to 20% higher than the number of positive carriers. Therefore it is to be assumed that the totality of the free charge carriers come into existence through interference of the effects of:

a) direct thermal emission from the metals;
b) partial ionization of a metallic vapor cloud liberated upon impact and produced as a result of the high temperature.

Interpretation of the dependence of the total charge measured on the projectile parameters of mass and velocity at first appears difficult, because there is not any proportionality to the kinetic energy of the incident particle. For this purpose the processes of particle impact must be considered more closely.

When a particle strikes, the orderly macroscopic movement of the particle

atoms is transferred into an unordered movement, which is seen in a rise in temperature at the place of impact. The height of temperature peak reached depends on the velocity v of the incident particle. According to Rudolph [5] an increase in stiking velocity causes an expansion of the crater volume proportional to v^2. Consequently the temperature at the point of time in which the incident energy is distributed over the crater volume is equal to all impact velocities. It should be identical with the solidification temperature of the target material. This is not in opposition to the assumption made above that at the beginning or during the course of the penetration process a higher peak temperature dependent on v is reached for a short time, because this does not prevail over the total crater volume. On the basis of this simplified approximation, the following picture can be given for the temporal course of impact and energy expansion:

The temperature in a narrowly limited vacinity of the impact place increases during penetration to a temperature peak dependent on v. Subsequently the temperature again drops because of energy expansion. On reaching vaporization temperature, the energy has expanded to a portion of space which will be designated with the name "volatile volume". Finally, upon reaching the melting point the energy fills the crater volume. Like the volatile volume, it is only dependent upon the energy of the incident particle. The fact that not only the expansion of energy in space, but also the vaporization, melting and deformation work help the temperature to sink, does not fundamentally alter anything about the existence of the above mentioned volumes. /35

The amount of liberated charges is dependent on the one hand upon the magnitude of the volatile volume. However, it is also correlated with the temperature peak reached upon impact. Vaporization is possible from the moment the vaporization point is exceeded until the temperature again goes below that point. The percentage portion of ionized atoms in this metallic vapor is dependent upon the temperature of this vapor. Since the magnitude of the volatile volume is proportional to energy $(1/2)mv^2$ and the temperature peak increases at the point of impact with increasing particle velocity, a velocity exponent, greater than 2, can be given. As a result of the experiments carried out, this situation is beyond doubt.

An explanatory remark is still necessary for the concept of "volatile volume". Since a target material is chosen with a very high boiling or vaporization point, it is preferable to deal with the vaporization of the project material. Thus it is reasonable to include with the volatile volume that portion of space in which the temperature is still capable of vaporizing the projectile found there.

The dependence of the charge emission on the angle of incidence of the projectile can be explained by assumptions similar to those used above. More complete discussion is given in 3.6.

The experimental findings obtained in Chapter 3 suggest the completion of the following requirements for the arrangement, calibration and execution of a flight experiment:

a) For optimum determination of the amount of charge liberated as complete a possible charge separation of the resultant plasma is required; this is provided in a satisfactory degree with the expansion of the plasma into a relatively large volume because of the smaller charge density.

b) A detector calibration of the form: $Q = \text{const } f(\Theta)\ m(v_{rel})$ is possible. However, the individual properties of every target surface to be struck must be determined directly. (e.g. the charge productivity of a tungsten target also depends on its previous history). The same is to be done for any screening foil used. /36

c) If possible, the determination or evaluation of the angle of incidence of a particle to be demonstrated in any single occurrence should not be neglected.

In judging the measurements from a flight experiment, other points of view should also be considered in the evaluation standard. These are:

d) In this work only laboratory experiments with the relatively heavy projectile material iron were carried out, while in flight experiments particles of a lesser density are to be dealt with. According to the measurements of Friichtenicht [7], the charge emission at fixed velocity is proportional to the number of atoms of the incident particle. In using only one projectile material, this is identical to a mass proportionality. The atoms in the Fe metal grid are relatively densely packed in comparison to other materials (non-metals such as C or Si compounds). For such non-metal particles, a lower charge emission per particle magnitude should therefore be expected.

e) The effect of any possible residue which can be connected with atmospheric pressure in front of the detector should not be considered in the relative detector-particle movement. This is definitely justified for satellite experiments, but has not yet been quantitatively investigated for rocket flights.

Finally let us mention one more reflection which makes sure that a supplementary spectrometric separation of the ions liberated on impact is reasonable. The fear that a mass spectrum obtained in this way does not reflect the chemical composition of the incident particle, but only its content in easily ionized elements (e.g. alkalis), can easily be done away with under certain suppositions. This comes from the fact that at high striking velocities a not inconsiderable ionization effect cross section occurs (see 3.3., Figure 10a). /37 Thus if a particle with a sufficiently high velocity strikes the target, it must be assumed that essential components in the composition of the particle will also make an essential contribution to the plasma cloud which evolves. The ions of the target material--the composition of which is known exactly--possibly present in the plasma are separated automatically by the spectrometer from the other kinds of ions. They are not considered in ascertaining the composition of the particle from the mass spectrum of the plasma. In addition, because of the high vaporization point of the target material, its vaporization

is possible only to a rather slight degree.

In experiments on satellites or probes, which leave the gravitational range of the earth, the following suppositions are made in contradistinction to rocket experiments:

1) long recording times;
2) absence of residue;
3) high relative particle-detector velocity.

Thus good mass sensitivity and a high ionization effect cross section are guaranteed which simplifies a supplementary mass spectrometric investigation of the incident matter.

Therefore it may be said that the proper area of use of a plasma detector is such satellite or probe experiments.

5. Summary

/38

The formation of free charge carriers when high energy microparticles impact upon a metallic collecter electrode offers suppositions for the recording of cosmic dust particles. The present work is concerned with this eventuality. In laboratory experiments the amounts of positive and negative charge Q^+ and Q^- liberated by the impact of Fe particles were investigated within the ranges of the following parameters:

$0.8\ \text{km/sec} < v < 40\ \text{km/sec}$; v = projectile velocity
$10^{-15}\text{g} < m < 5 \times 10^{-10}\text{g}$; m = projectile mass

The measurements in this work were carried out on a 2MV Van de Graaff particle accelerator of the Institute. Here we wished to determine the dependence of the charge emissions on

1) the projectile parameters (charge, mass, velocity and angle of incidence of the particle),
2) target properties (degree of impurity in alkalis, general surface condition),
3) external experimental conditions at and in front of the impact spot (electrical field strength, detector geometry, use of a foil to be penetrated by the particle).

From the experiments carried out the following conditions are inferred:

1a) the amount of charge liberated is independent of the charge condition of the particle
b) it is approximately proportional to the incident mass.

$$Q \sim m^{\alpha} \quad ; \quad \alpha \simeq 1 \text{ for } 0{,}8\ \text{km/sec} < v < 2\ \text{km/sec}$$
$$\alpha \simeq 0.9 \text{ for } 2\ \text{km/sec} < v < 9\ \text{km/sec}$$

c) the quotient Q/m vanishes below a limiting velocity of 0.8 km/sec. In the range of 2-9 km/sec the following is valid:

$$Q \sim m^{(0,9 \pm 0,15)}\ v^{(2,7 \pm 0,4)}$$

Between 30 and 40 km/sec the number of elementary charges liberated reaches values from 5% to 20% of the number of atoms in the incident projectile.

d) the charge emission is dependent on the angle of incidence of the particle in a manner characteristic of the target, with a maxiumum emission occurring at about 45°.

2) tungsten targets of various production or pretreatment have various charge productivities up to 20%.

3a) the measurement of the charge emission is made easier if the charge carrier of the plasma cloud originating in the impact can be expanded by diffusion into a sufficiently large volume which is still completely inside the charge-separating field. By using a plane detector system, a distance of about 1cm between target and electrically stressed collecting grid is measured. /39

b) in the choice of a foil to screen out external influences, a compromise must be reached between particle penetrability and mechanical resistance. A nitrocellulous foil, 0.2 to 0.4μ thick, was well suited for Fe particles in this respect.

From these findings it turns out that the calibration of a plasma detector is characterized by an equation of the following type:

$$Q = \text{const} \quad f(\Theta) \quad m^{\alpha} \, (v_{rel})^{\beta} \, .$$

Attention is to be given here to the individual properties of the special target surfaces and any screening foil used.

This method of recording cosmic particles seems to be promising, particularly in respect to satellite experiments and for interplanetary probes. The decisive advantages of these methods are used in the best possible way only with high relative velocities between the detector and the particles to be demonstrated. These are the high mass sensitivity and the possibility of spectrometric investigation of the liberated ions.

6. REFERENCES /40

1. Elsasser, H., "The Spatial Distribution of the Zodiacal Light Material", *Z. Astrophys.*, Number 33, 1954.
2. Schmidt, R. A., "Microscopic Extraterrestrial Particles from the Antarctic Peninsula Traverse", *Res. Rep.*, Series 63-3, July, 1963.
3. Millman and McIntosh, "Meteor Radar Statistics", *Can. Journ. of Phys.*, Volume 44, 1953.
4. Alexander, W. M., C. W. McCracken, L. Secretan and O. E. Berg, "Review of Direct Measurements of Interplanetary Dust from Satellites and Probes", *Space Res.*, Number 3, p. 891, 1963.
5. Rudolph, V., *Dissertation*, University of Heidelberg, 1967.
6. Fechtig, H., U. Gerloff, and J. H. Weihrauch, "Results of Cosmic Dust Collection on Luster 1965", *J. Geophys. Res.*, Volume 73, p. 5029, 1968.

7. Friichtenicht, J. F. and J. C. Slattery, "Ionization Associated with Hypervelocity Impact", *NASA Technical Note D-2091*.
8. Auer, S., *Dissertation*, University of Heidelberg, 1967.
9. Alexander, W. M. and J. Lloyd Bohn, "Zodiacal Dust Measurements in Cis-Lunar and Interplanetary Space from OGO III and Mariner IV Experiments Between June and December 1966", *Space Res.*, Number 8, p. 489.
10. Shelton, H., C. D. Hendricks, Jr. and R. F. Wuerker, "Electrostatic Acceleration of Microparticles of Hypervelocities", *Journ. Appl. Phys.*, Volume 31, 1960.
11. Friichtenicht, J. F., "Two-Million Volt Electrostatic Accelerator for Hypervelocity Research", *Rev. Sci. Instr.*, Volume 33, 1962.
12. Rudolph, V. "Mass Velocity Filter for Artifically Accelerated Dust", *Z. Natur.* 21a, 1966.

ACKNOWLEDGEMENTS /41

My special thanks go to Professor Doctor W. Gentner for the possibility of carrying out this work at his Institute.

I thank Professor Doctor J. Zahringer for support in this work.

I acknowledge my thanks to Professors Doctor K. Sitte, Doctor H. Fechtig, Doctor S. Auer, Doctor P. Rauser, Doctor V. Rudolph and Doctor M. Feuerstein for many discussions and suggestions.

I would also like to thank Mr. E. Grun, Dipl. Phys., and Mr. G. Neukum for their fine cooperation and for numerous valuable conversations.

In addition I must thank a great many of the members of the Institute, particularly operators and workers, for the help they made available to me.

Translated for the National Aeronautics and Space Administration under contract No. NASw-1695 by Techtran Corporation, P.O. Box 729, Glen Burnie, Maryland 21061